

Numerical methods for the computation of the confluent and Gauss hypergeometric functions

John W. Pearson¹ · Sheehan Olver² ·
Mason A. Porter³

Received: 27 August 2015 / Accepted: 29 June 2016 / Published online: 27 August 2016
© Springer Science+Business Media New York 2016

Abstract The two most commonly used hypergeometric functions are the confluent hypergeometric function and the Gauss hypergeometric function. We review the available techniques for accurate, fast, and reliable computation of these two hypergeometric functions in different parameter and variable regimes. The methods that we investigate include Taylor and asymptotic series computations, Gauss–Jacobi quadrature, numerical solution of differential equations, recurrence relations, and others. We discuss the results of numerical experiments used to determine the best methods, in practice, for each parameter and variable regime considered. We provide “roadmaps” with our recommendation for which methods should be used in each situation.

Keywords Computation of special functions · Confluent hypergeometric function · Gauss hypergeometric function

This work was supported by the Numerical Algorithms Group (NAG) and the Engineering and Physical Sciences Research Council (EPSRC).

✉ John W. Pearson
j.w.pearson@kent.ac.uk

Sheehan Olver
Sheehan.Olver@sydney.edu.au

Mason A. Porter
porterm@maths.ox.ac.uk

¹ School of Mathematics, Statistics and Actuarial Science, University of Kent, Cornwallis Building (East), Canterbury, Kent, CT2 7NF, UK

² School of Mathematics and Statistics, The University of Sydney, NSW 2006, Sydney, Australia

³ Oxford Centre for Industrial and Applied Mathematics, Mathematical Institute, University of Oxford, Andrew Wiles Building, Radcliffe Observatory Quarter, Woodstock Road, Oxford, OX2 6GG, UK

Mathematics Subject Classification (2010) Primary: 33C05 · 33C15 · Secondary: 41A58 · 41A60

1 Introduction

The aim of this review paper is to summarize methods for computing the two most commonly used hypergeometric functions: the confluent hypergeometric function $\mathbf{M}(a; b, z)$ and the Gauss hypergeometric function $\mathbf{F}(a, b; c; z)$. (We also consider the associated functions ${}_1F_1(a; b; z)$ and ${}_2F_1(a, b; c; z)$.) We overview methods that have been developed for computing \mathbf{M} and \mathbf{F} , and we discuss how to choose appropriate methods for different parameter and variable regimes. We thereby obtain reliable and fast computation for a large range of the parameters (a and b for \mathbf{M} ; and a , b , and c for \mathbf{F}) and the variable z . Because accurate error bounds are seldomly available, we test a large variety of approaches, which we require to be stable, accurate, fast, and robust within the parameter and variable regions for which they have been selected. This is especially important when working with finite-precision arithmetic.

The computation of confluent hypergeometric functions and Gauss hypergeometric functions is important in a wide variety of applications [87]. For instance, these functions arise in areas such as photon scattering from atoms [27], networks [79, 100], Coulomb wave functions [8, 21, 67], binary stars [81], mathematical finance [10], non-Newtonian fluids [109], and more.

Except for specific situations, computing hypergeometric functions is difficult in practice. A plethora of methods exist for computing each hypergeometric function; these include Taylor series, asymptotic expansions, continued fractions, recurrence relationships, hyperasymptotic expansions, and more. However, each method is only reliable and efficient for limited parameter and variable regimes. Consequently, one must be prepared to use different members of this suite of possibilities in different regimes of parameter and variable values.

We have also developed MATLAB code for computing the functions \mathbf{M} and \mathbf{F} using a range of methods; our code is publicly available [116].

2 Background on hypergeometric functions

The confluent hypergeometric function is defined by [110, Eq. (13.2.3)]

$$\mathbf{M}(a; b; z) = \sum_{j=0}^{\infty} \frac{(a)_j}{\Gamma(b+j)} \frac{z^j}{j!}, \quad (2.1)$$

where the *Pochhammer symbol* $(\mu)_j$ is

$$(\mu)_0 = 1, \quad (\mu)_j = \mu(\mu+1) \times \cdots \times (\mu+j-1), \quad j = 1, 2, \dots$$

The function \mathbf{M} is entire (i.e., it is analytic throughout the complex plane \mathbb{C}) in the parameters a and b and the variable z . Therefore, the sum (2.1) always converges.

When b is not a non-positive integer, we define

$${}_1F_1(a; b; z) = \Gamma(b)\mathbf{M}(a; b; z) = \sum_{j=0}^{\infty} \frac{(a)_j z^j}{(b)_j j!},$$

which is also commonly denoted by $M(a; b; z)$ and is itself often called the confluent hypergeometric function. Because ${}_1F_1(a; b; z)$ is not defined if b is equal to a non-positive integer and there are numerical issues in its computation if b is close to a non-positive integer, it is preferable to compute \mathbf{M} when possible.

The Gauss hypergeometric function is defined within the unit disk $|z| < 1$ by [110, Eq. (15.2.2)]

$$\mathbf{F}(a, b; c; z) = \sum_{j=0}^{\infty} \frac{(a)_j (b)_j z^j}{\Gamma(c + j) j!} \tag{2.2}$$

and defined outside the unit disk by analytic continuation, with a principal branch cut along $[1, \infty)$. On $[1, \infty)$, it is defined to be continuous from below. That is, $\mathbf{F}(a, b; c; z) = \lim_{\epsilon \rightarrow 0} \mathbf{F}(a, b; c; z - |\epsilon|i)$. When c is not a non-positive integer, we define

$${}_2F_1(a, b; c; z) = \Gamma(c)\mathbf{F}(a, b; c; z) \left(= \sum_{j=0}^{\infty} \frac{(a)_j (b)_j z^j}{(c)_j j!} \text{ for } |z| < 1 \right). \tag{2.3}$$

The function ${}_2F_1(a, b; c; z)$ is commonly denoted by $F(a, b; c; z)$ and is also frequently called the Gauss hypergeometric function. Analogous to the case for the confluent hypergeometric function, it is better numerically to compute \mathbf{F} than to compute ${}_2F_1$.

The confluent hypergeometric function ${}_1F_1(a; b; z)$ satisfies the ordinary differential equation [90]

$$z \frac{d^2 f}{dz^2} + (b - z) \frac{df}{dz} - af = 0, \tag{2.4}$$

and the Gauss hypergeometric function ${}_2F_1(a, b; c; z)$ satisfies [91]

$$z(1 - z) \frac{d^2 f}{dz^2} + [c - (a + b + 1)z] \frac{df}{dz} - abf = 0. \tag{2.5}$$

The confluent and Gauss hypergeometric functions are examples of *special functions*, whose theory and computation are prominent in the scientific literature [3, 6, 40, 53, 57, 58, 62, 73, 95, 97, 108]. A large number of common mathematical functions (including e^z , $(1 - z)^{-a}$, and $\sin^{-1} z$ [3, 57]) and many special functions (such as the modified Bessel function, the incomplete gamma and error functions, Chebyshev and Legendre polynomials, and other families of orthogonal polynomials [3, 5, 60, 85]) can be expressed in terms of confluent or Gauss hypergeometric functions.

In Figs. 1 and 2, we show plots of hypergeometric functions. These provide examples of the possible shapes of such functions in the real and complex planes, though of course there are a wide range of possible representations of them.

As we indicated above, the computation of hypergeometric functions arises in a wide variety of applications. This underscores the importance of determining which

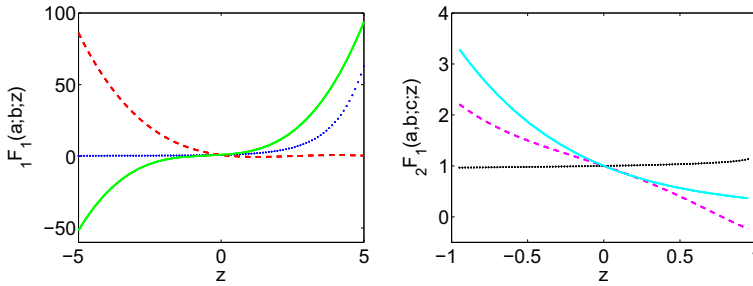


Fig. 1 (Color online) (Left) Plots of ${}_1F_1(a; b; z)$, generated using MATLAB [111], for real $z \in [-5, 5]$ with parameter values $(a, b) = (0.1, 0.2)$ in dark blue (dotted), $(a, b) = (-3.8, 1.5)$ in red (dashed), and $(a, b) = (-3, -2.5)$ in green (solid). (Right) Plots of ${}_2F_1$ for real $z \in [-1, 1]$ with parameter values $(a, b, c) = (0.1, 0.2, 0.4)$ in black (dotted), $(a, b, c) = (-3.6, -0.7, -2.5)$ in purple (dashed), and $(a, b, c) = (-5, 1.5, 6.2)$ in sky blue (solid)

computational techniques are accurate and efficient for different parameter and variable regimes. It is also important to supply information on how to test the reliability of a routine, provide test cases that a routine might have difficulty computing (see Appendix A), and indicate how to evaluate other special functions required for the computation of hypergeometric functions (see Appendix C). As illustrated in Ref. [80], the inbuilt routines to compute hypergeometric functions in commercial software packages such as MATLAB R2015a [111] and Mathematica 8 [112] are not without limitations, so one should not rely on them in many parameter and variable regimes. We have implemented our routines for MATLAB R2015a, which uses double-precision arithmetic, and we have made it freely available online [116]. Of course, it is easier to obtain accurate results when computing these functions in higher-precision arithmetic, as is done when the inbuilt hypergeometric function commands in MATLAB and MATHEMATICA are called. Our code can be modified to run in higher precision.

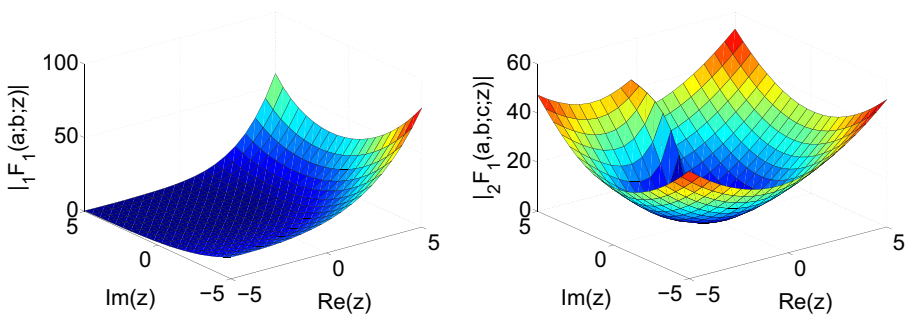


Fig. 2 (Color online) (Left) Plot of $|{}_1F_1(a; b; z)|$ for $(\text{Re}(z), \text{Im}(z)) \in [-5, 5]^2$ with parameter values $(a, b) = (-3 - 2i, 2.5)$. (Right) Plot of $|{}_2F_1|$ for $(\text{Re}(z), \text{Im}(z)) \in [-5, 5]^2$ with parameter values $(a, b, c) = (1 + 2i, -1.5, 0.5 - i)$

3 Computation of the confluent hypergeometric function \mathbf{M}

In this section, we discuss the methods that perform the best in practice for accurately and efficiently evaluating the confluent hypergeometric function. The range of methods that we discuss includes series computation methods (Sections 3.2, 3.3, and 3.4), quadrature methods (Section 3.5), recurrence relations (Section 3.6), and other methods (Section 3.7). In Section 3.8, we summarize the computational strategies and provide recommendations for the most effective approaches for a variety of parameter regimes.

3.1 Properties of \mathbf{M}

As stated in Section 2, the confluent hypergeometric function $\mathbf{M}(a; b; z)$ is defined by the series (2.1) for any $a \in \mathbb{C}, b \in \mathbb{C}$, and $z \in \mathbb{C}$. We note that $\mathbf{M}(a; b; 0) = \frac{1}{\Gamma(b)}$. Additionally, if $a = n \in \mathbb{Z}^- \cup \{0\}$, then this series is given by a polynomial in z of degree $-n$.

A second, linearly independent solution of equation (2.4) is denoted $U(a; b; z)$ and is defined by the property that $U(a; b; z) \sim z^{-a}$ as $|z| \rightarrow \infty$ for $|\arg z| \leq \frac{3}{2}\pi - \delta$, with $0 < \delta \ll 1$ [57]. The function $U(a; b; z)$ satisfies [3]

$$U(a; b; z) = \frac{\pi}{\sin(\pi b)} \left(\frac{1}{\Gamma(1 + a - b)} \mathbf{M}(a; b; z) - \frac{z^{1-b}}{\Gamma(a)} \mathbf{M}(1 + a - b; 2 - b; z) \right).$$

The function $U(a; b; z)$ is defined with a principal branch cut along $(-\infty, 0]$. When $m \in \mathbb{Z}$, one obtains [110, Eq. (13.2.12)]

$$U(a; b; ze^{2\pi im}) = \frac{2\pi i e^{-\pi ibm} \sin(\pi bm)}{\Gamma(1 + a - b) \sin(\pi b)} \mathbf{M}(a; b; z) + e^{-2\pi ibm} U(a; b; z).$$

The functions $\mathbf{M}(a; b; z)$ and $U(a; b; z)$ are related by [98]

$$\mathbf{M}(a; b; z) = \frac{e^{\mp a\pi i}}{\Gamma(b - a)} U(a; b; z) + \frac{e^{\pm(b-a)\pi i}}{\Gamma(a)} e^z U(b - a; b; e^{\pm\pi i} z). \tag{3.1}$$

Therefore, methods for computing $U(a; b; z)$ can also be useful for computing \mathbf{M} , and vice-versa, provided one is careful about numerical issues such as cancellation. One can also exploit methods for computing ${}_1F_1$ in conjunction with the above expressions, as well as the transformation [110, Eq. (13.2.39)]

$${}_1F_1(a; b; z) = e^z {}_1F_1(b - a; b; -z) \Leftrightarrow \mathbf{M}(a; b; z) = e^z \mathbf{M}(b - a; b; -z), \tag{3.2}$$

which enables one to handle a change in $\text{sign}(z)$.

There are many useful applications of the confluent hypergeometric function. For example, it has been used to find exact solutions of the wave equation [40], obtain insights on the scattering of charged particles [8], analyze gene-frequency data [102], and investigate Asian options in finance [10].

3.2 Taylor series

The simplest method for computing the confluent hypergeometric function is to truncate the Taylor series

$${}_1F_1(a; b; z) \approx S_N = \sum_{j=0}^N \underbrace{\frac{(a)_j}{(b)_j} \frac{1}{j!}}_{A_j} z^j, \tag{3.3}$$

and then use the relation ${}_1F_1(a; b; z) = \Gamma(b)\mathbf{M}(a; b; z)$.

A *stopping criterion* must be specified. It is common to stop computing terms when $\frac{|A_{N+1}|}{|S_N|} < \text{tol}$ for some tolerance tol and some N , and then return S_N (our approximation of ${}_1F_1(a; b; z)$) as the solution [63]. Alternatively, one can terminate computation of the series using the more stringent condition that two successive terms are small. We use this latter approach in our numerical experiments.

By taking $\text{tol} = \text{eps}$, we obtain an accuracy of approximately 15 decimal places (if round-off error does not play a role). Note that $\text{eps} \approx 2.2 \times 10^{-16}$ denotes “machine epsilon” in MATLAB. We choose this value for tol for all of the series computations in this paper.

Even the simple task of summing the Taylor series can be accomplished in different ways, and this can have a significant impact on stability and efficiency. We consider two methods for computing S_N .

Method (a) Compute

$$\begin{aligned} A_0 &= 1, & S_0 &= A_0, \\ A_{j+1} &= A_j \frac{a+j}{b+j} \frac{z}{j+1}, & S_{j+1} &= S_j + A_{j+1}, \quad j = 0, 1, 2, \dots \end{aligned}$$

Method (b) The following three-term recurrence relation can be used to obtain approximations of $M(a; b; z)$ recursively in terms of previous approximations [63]:

$$\begin{aligned} S_{-1} &= S_0 = 1, & S_1 &= 1 + \frac{a}{b}z, \\ r_j &= \frac{a+j-1}{j(b+j-1)}, & S_j &= S_{j-1} + (S_{j-1} - S_{j-2})r_jz, \quad j = 2, 3, \dots \end{aligned}$$

As one can see in Table 9 in Appendix B, Methods (a) and (b) generate similar results and require the same number of terms for most computations. However, as also illustrated by Table 9, Method (b) is in general more effective when carrying out computations involving small parameters.

By examining the coefficients of the series, we see that S_N converges particularly quickly when z is close to 0 or when b has a large real part and a relatively small imaginary part (because $\Gamma(\cdot)^{-1}$ decays rapidly near the positive real axis); again see Table 9. We note that (3.3) can be viewed as an asymptotic expansion for large values of $|b|$ and bounded a, z , which explains this feature. However, as a or z becomes large, the coefficients of the Taylor series become large, slowing down the convergence rate (see Fig. 3). See Table 9, where the

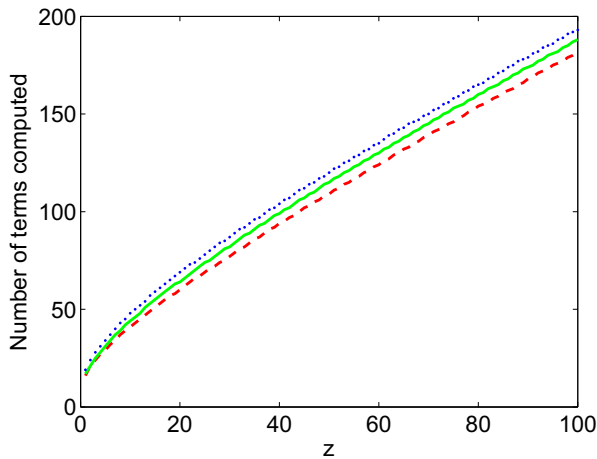


Fig. 3 (Color online) Number of terms that need to be computed using Taylor series Method (a) for evaluating ${}_1F_1$ (and hence \mathbf{M}) for real $z \in [1, 100]$ when $a = 2$ and $b = 3$ (red, dashed), $a = 2 + 10i$ and $b = 10 + 5i$ (green, solid), and $a = 20$ and $b = 15$ (blue, dotted) before the stopping criterion (two successive small terms) is satisfied. The method gives results to 15-digit accuracy

Taylor series is accurate up to and even beyond $|z| = 100$ (although the approximation becomes less accurate as $|z| \rightarrow \infty$), depending on the parameter values involved.

As demonstrated by cases 13–16 in Table 9, a significant issue with computing \mathbf{M} using Taylor series is cancellation. Although $|a|$ and $|z|$ are the same in each of these cases, a Taylor series method is effective in these cases if a and z have the same signs, whereas it is ineffective if their signs are different. In this situation, we find that the Buchholz polynomial expansion that we describe in Section 3.3 is more effective.

3.2.1 Writing S_N as a single fraction

As illustrated by the performance of Taylor series Method (a) on cases such as $(a, b, z) = (10^{-8}, 10^{-12}, -10^{-10} + 10^{-12}i)$, where machine-precision accuracy is not attained despite the apparent simplicity of the parameter regime (in the sense that we expect many methods to be both fast and accurate), the methods of Section 3.2 can often have significant inaccuracies when the parameter values have small moduli, even though one might naïvely expect the computation to be fairly straightforward. The method that we discuss in this section aims to provide an alternative to those in Section 3.2. It is also based on the basic series definition (2.1) of the confluent hypergeometric function [64, 65].

The motivation behind this method is that significant round-off error can arise when repeatedly dividing during the computation of individual terms of a Taylor series using other methods. Therefore, applying a method that only requires a single division to compute an approximation to ${}_1F_1(a; b; z)$ is potentially advantageous.

In this method, we express the series expansion of ${}_1F_1(a; b; z)$ as a single fraction rather than as a sum of many fractions. For example, the sum S_j of the first $j + 1$ terms of the series up to the term in z^2 can be expressed as

$$S_0 = \frac{0 + 1}{1}, \quad S_1 = \frac{b + az}{b}, \quad S_2 = \frac{(b + az)2(b + 1) + a(a + 1)z^2}{2b(b + 1)},$$

where the numerators and denominators of S_0, S_1, S_2, \dots can be calculated using (3.4). If we take $\alpha_0 = 0, \beta_0 = 1, \gamma_0 = 1$, and $S_0 = 1$ and define S_j to be the j th approximation of ${}_1F_1(a; b; z)$, we can apply the following algorithm:

Method (c)

$$\begin{aligned} \alpha_j &= (\alpha_{j-1} + \beta_{j-1})j(b + j - 1), \\ \beta_j &= \beta_{j-1}(a + j - 1)z, \\ \gamma_j &= \gamma_{j-1}j(b + j - 1), \\ S_j &= \frac{\alpha_j + \beta_j}{\gamma_j}, \quad j = 1, 2, \dots \end{aligned} \quad (3.4)$$

Implementing this method generates a sequence of approximations to ${}_1F_1(a; b; z)$ (i.e., approximations of S_j for $j = 1, 2, \dots$), which we terminate using the same stopping criterion as in Section 3.2.

From Table 9, one can conclude that Methods (a) and (b) generate accurate computations of $\mathbf{M}(a; b; z)$ more successfully than Method (c) for a wide range of parameter and variable values. One possible explanation for this—especially as the moduli of the parameter values become increasingly large—is that the terms in the numerator and denominator of S_j become very large for relatively small j , so numerical issues such as round-off error and cancellation can become significant when carrying out the computations. Additionally, we often find that either the numerator or the denominator of S_j becomes very large after only a few summations. Nevertheless, we observe that Method (c) can be useful if $|b|$ is small (especially when $|b| \lesssim 1$), provided $|a|$ is not too large, whereas if one uses Methods (a) and (b) when $|b|$ is small, the round-off error can become costly if many terms are too large. Therefore, a method with a single division can potentially aid accurate computation in this case, as the effect of round-off error is reduced.

To illustrate many of the effects observed in this section, in Table 1 we present a handful of examples for which one method performs significantly worse than the other two. This highlights the need to take care when selecting an appropriate strategy, in particular for small parameters (when Method (a) in particular can be less effective) and large values of $|z|$ (when Method (c) struggles for the reasons explained above).

3.3 Buchholz polynomials

References [1, 2] used Buchholz polynomials to derive expressions for $\mathbf{M}(a; b; z)$, focusing on the regime of real parameters and a real variable. We find that this yields

Table 1 Computed values of $\mathbf{M}(a; b; z)$ using Methods (a), (b), and (c) for several examples and fixed numbers N of computed terms. Incorrect digits are written in bold

(a, b, z)	$(-0.1, 0.2, 0.5)$	$(4, 8, 200)$	$(10, 10^{-12}, 10)$
N	20	350	60
(a)	0.151505171758381	$7.086610326129021 \times 10^{76}$	$1.332415988221994 \times 10^{11}$
(b)	0.151505171758381	$7.086610326129031 \times 10^{76}$	$1.332534440779267 \times 10^{11}$
(c)	0.151505171758381	$9.020181831462336 \times 10^{56}$	$1.332534440779269 \times 10^{11}$
(a, b, z)	$(10^{-8}, 10^{-12}, -10^{-10} + 10^{-12}i)$	$(8.1, 10.1, 100)$	
N	30	200	
(a)	$9.999990000894761 \times 10^{-13}$ $+9.999111011439252 \times 10^{-21}i$	$3.791292609415422 \times 10^{35}$	
(b)	$9.99999000005772 \times 10^{-13}$ $+9.99999999005773 \times 10^{-21}i$	$3.791292609415425 \times 10^{35}$	
(c)	$9.99999000005768 \times 10^{-13}$ $+9.99999999005770 \times 10^{-21}i$	$3.174500309594823 \times 10^{34}$	

a much more effective approach than the methods discussed in Section 3.2 for the computation of $\mathbf{M}(a; b; z)$ when $\text{sign}(a) = -\text{sign}(z)$.

The function $\mathbf{M}(a; b; z)$ can be expanded in terms of Buchholz polynomials $p_j(b, z)$ as follows:

$$\mathbf{M}(a; b; z) = e^{z/2} 2^{b-1} \sum_{j=0}^{\infty} p_j(b, z) \frac{J_{b-1+j}(\sqrt{z\{2b-4a\}})}{(z\{2b-4a\})^{\frac{1}{2}(b-1+j)}} \tag{3.5}$$

provided $b \neq 2a$; when $b = 2a$, one obtains [3]

$$\mathbf{M}(a; 2a; z) = \frac{\Gamma\left(a + \frac{1}{2}\right)}{\Gamma(2a)} e^{z/2} \left(\frac{iz}{4}\right)^{-(a-\frac{1}{2})} J_{a-\frac{1}{2}}\left(\frac{iz}{2}\right),$$

where $J_\nu(z)$ denotes the Bessel function of the first kind. The coefficients of (3.5) are

$$p_j(b, z) = \frac{(iz)^j}{j!} \sum_{s=0}^{\lfloor \frac{j}{2} \rfloor} \binom{j}{2s} f_s(b) g_{j-2s}(z), \tag{3.6}$$

where

$$f_0(b) = 1, \quad f_s(b) = -\left(\frac{b}{2} - 1\right) \sum_{j=0}^{s-1} \binom{2s-1}{2j} \frac{4^{s-j} |B_{2(s-j)}|}{s-j} f_j(b), \quad s = 1, 2, \dots,$$

$$g_0(z) = 1, \quad g_s(z) = -\frac{iz}{4} \sum_{j=0}^{\lfloor \frac{s-1}{2} \rfloor} \binom{s-1}{2j} \frac{4^{j+1} |B_{2(j+1)}|}{j+1} g_{s-2j-1}(z), \quad s = 1, 2, \dots$$

The coefficients B_j denote the *Bernoulli numbers*, which are defined by the generating function

$$\frac{z}{e^z - 1} = \sum_{j=0}^{\infty} B_j \frac{z^j}{j!}.$$

A more convenient form of (3.5), which utilizes recurrence relations for the Buchholz polynomials, for real a (there are no such restrictions on the values of b and z) is as follows [2]:

$$\mathbf{M}(a; b; z) = e^{z/2} 2^{b-1} \sum_{j=0}^{\infty} D_j z^j \frac{J_{b-1+j}(\sqrt{z\{2b-4a\}})}{(z\{2b-4a\})^{\frac{1}{2}(b-1+j)}}, \quad (3.7)$$

where

$$D_0 = 1, D_1 = 0, D_2 = \frac{b}{2}, \\ jD_j = (j-2+b)D_{j-2} + (2a-b)D_{j-3}, \quad j = 3, 4, \dots \quad (3.8)$$

The expression in (3.7) is the series that we implement in our code and provides an expansion for the confluent hypergeometric function in terms of Bessel functions, which are significantly easier to compute than \mathbf{M} . We evaluate terms of (3.7) until the magnitudes of two successive terms are smaller than ϵ_{ps} multiplied by the magnitude of the computed series up to that point. (We typically compute the Bessel functions using series expansions with the same stopping conditions as for \mathbf{M} in Section 3.2; see Appendix C for more details.)

As illustrated in Table 9, this method seems to outperform the Taylor series methods of Section 3.2 for computation of \mathbf{M} for certain parameter regimes, and this is particularly true for many examples in which $\text{sign}(a) \neq \text{sign}(z)$. The method is also valuable for moderate complex values of a and z (in particular, for $10 \lesssim |a|, |z| \lesssim 100$), especially when the real parts of a and z have opposite signs. The Taylor series methods discussed in Section 3.2 and the single-fraction method of Section 3.2.1 do not give accurate computations with these cases, but the method described in this section performs very well. (See Table 9 in Appendix B.) One even obtains a very accurate result when $|a|$ is large (e.g., when $|a| = 500$), with real z of opposite sign to that of a . (See case 19 in Appendix A, for which we obtain 16-digit accuracy.) As illustrated in Appendix B, however, this method becomes less successful as $|z|$ becomes larger. Nonetheless, the good performance of this method for a large range of parameter values makes it a convenient element of one's toolbox for computing $\mathbf{M}(a; b; z)$.

3.4 Asymptotic series for large $|z|$

The methods that we outlined in Sections 3.2 and 3.3 were all ineffective (in general) for large values of $|z|$. (We found that these methods ceased to be effective for $|z| \gtrsim 100$, although the threshold was sometimes lower, depending on the precise values of the parameters.) In this section, we aim to address this issue by using large- $|z|$ asymptotic formulas for computing the confluent hypergeometric function.

One can apply Watson’s lemma [104] to show that as $|z| \rightarrow \infty$, the hypergeometric function $\mathbf{M}(a; b; z)$ satisfies [3]

$$\mathbf{M}(a; b; z) \sim \frac{e^z z^{a-b}}{\Gamma(a)} \sum_{j=0}^{\infty} \frac{(b-a)_j (1-a)_j}{j!} z^{-j} + \frac{e^{\pm \pi i a} z^{-a}}{\Gamma(b-a)} \sum_{j=0}^{\infty} \frac{(a)_j (1+a-b)_j}{j!} (-z)^{-j}, \tag{3.9}$$

where $a, b \in \mathbb{C}$, $-\frac{1}{2}\pi + \delta \leq \pm \arg z \leq \frac{3}{2}\pi - \delta$,¹ and $0 < \delta \ll 1$.

The expression when z is real and positive is [110, Eq. (13.7.1)]

$$\mathbf{M}(a; b; z) \sim \frac{e^z z^{a-b}}{\Gamma(a)} \sum_{j=0}^{\infty} \frac{(b-a)_j (1-a)_j}{j!} z^{-j},$$

provided $a \notin \mathbb{Z}^- \cup \{0\}$.

We compute these series in MATLAB using the same two techniques as for the Taylor series expansion in Section 3.2. In the first method, we compute each term by adding each new term recursively to the previous sum, where we continue including new terms until they become small and apply the same stopping criterion as before. In the second method, we find each term iteratively in terms of the previous two terms and then add the new term to the previous sum. As in Section 3.2, we label these techniques as Methods (a) and (b). We show our results in Table 9.

As with the Taylor series techniques of Section 3.2, we obtain similar results using Methods (a) and (b). Both methods work well for large $|z|$ and moderate values of the parameters a and b .

Because the asymptotic series are expressed in terms of hypergeometric series of the form ${}_2F_0$ instead of ${}_1F_1$ (or \mathbf{M}), there is no longer a $(b)_j$ term in the denominator of the terms of the series, so parameter regimes involving b with large modulus can no longer be treated in a straightforward manner.² The cases that we tested suggest that the methods cope reasonably well when neither $|a|$ nor $|b|$ is very large. (As a guide, the computations seem to lose accuracy when $|a|$ or $|b|$ is greater than 50, although this depends on the value of z . For these cases, one needs to apply recurrence relations; see the discussion in Section 3.6 [65, 66].)

Other research into asymptotic formulas for the confluent hypergeometric function includes a discussion in Refs. [68, 74, 77] of an expansion

$$U(a; b; z) = z^{-a} \sum_{j=0}^{N-1} \frac{(a)_j (a-b+1)_j}{j!} (-z)^{-j} + R_N(a; b; z) \tag{3.10}$$

¹As in [3], when we write “ \pm ”, the sign “+” is used if $-\frac{1}{2}\pi < \arg z < \frac{3}{2}\pi$, and “-” is used if $-\frac{3}{2}\pi < \arg z < \frac{1}{2}\pi$. The argument is assigned the limits $\pm(\frac{3}{2}\pi - \delta)$ and $\pm(-\frac{1}{2}\pi + \delta)$ to ensure validity of the expansion over the branch cut.

²We define the hypergeometric function ${}_2F_0$ as follows:

$${}_2F_0(a, b; -; z) = \sum_{j=0}^{\infty} (a)_j (b)_j \frac{z^j}{j!}.$$

that one can use to compute \mathbf{M} via the expression (3.1). A *uniform, exponentially improved asymptotic expansion* is derived in [74, 77], and a second expansion with this property is derived in Ref. [68]. This was in turn extended in Ref. [72] to a *hyperasymptotic expansion*, which offers another possibility for computing \mathbf{M} for large $|z|$.

There has also been research on uniform asymptotic expansions of $\mathbf{M}(a; b; z)$ for large, real values of the parameters a and b . For example, reference [98] derived an expansion for large (real and positive) values of b and z in terms of parabolic cylinder functions. (We discuss methods for computing parabolic cylinder functions in Appendix C.) Reference [99] gave an expansion for $U(a; b; z)$ for large values of a (which must be real and positive) and $b \leq 1$ in terms of modified Bessel functions (which are themselves expressible in terms of Bessel functions [110]). We also recommend the new book [92] for a summary of asymptotic results for the confluent hypergeometric function.

3.5 Quadrature methods

Thus far, we have only considered methods based on series. In this section, we discuss a class of methods for computing $\mathbf{M}(a; b; z)$ using its integral representation for $a, b \in \mathbb{R}$ with $b > a > 0$.

When $\text{Re}(b) > \text{Re}(a) > 0$, the function $\mathbf{M}(a; b; z)$ has the integral representation [3]

$$\mathbf{M}(a; b; z) = \frac{1}{\Gamma(a)\Gamma(b-a)} \int_0^1 e^{zt} (1-t)^{b-a-1} t^{a-1} dt. \tag{3.11}$$

Applying the transformation $t \mapsto \frac{1}{2}\tilde{t} + \frac{1}{2}$ and using the Jacobi parameters $\tilde{\alpha} = b - a - 1$ and $\tilde{\beta} = a - 1$, for real $b > a > 0$, yields [26]

$$\begin{aligned} \mathbf{M}(a; b; z) &= \frac{1}{2^{b-1}\Gamma(a)\Gamma(b-a)} \int_{-1}^1 e^{z(\frac{1}{2}\tilde{t} + \frac{1}{2})} (1-\tilde{t})^{b-a-1} (1+\tilde{t})^{a-1} d\tilde{t} \\ &= \frac{1}{\Gamma(a)\Gamma(b-a)} \left[\frac{e^{z/2}}{2^{b-1}} \sum_{j=1}^{N_{\text{mesh}}} w_j^{GJ} e^{zt_j^{GJ}/2} + E_{N_{\text{mesh}}}(a; b; z) \right], \end{aligned}$$

where t_j^{GJ} and w_j^{GJ} are (respectively) the Gauss–Jacobi nodes and weights on $[-1, 1]$ and N_{mesh} is the number of mesh points.

This method is known as *Gauss–Jacobi quadrature*. The error $E_{N_{\text{mesh}}}$ for this method can be controlled by N_{mesh} , which one can determine for real a, b , and z using the following relation [26]:

$$N_{\text{mesh}} \geq \frac{e|z|}{8} \tilde{t} \left(\frac{4}{e|z|} \left[z_+ + (3-2b) \log 2 + \log \left(\frac{1}{E_{N_{\text{mesh}}}} \right) \right] \right), \tag{3.12}$$

where z_+ is equal to z if $z \geq 0$ and is equal to 0 if it is negative. The quantity \tilde{t} denotes the inverse of the function $s = \tilde{t} \log \tilde{t}$. Low-order approximations are given in Ref. [26] for different real values of s . To illustrate the results of this bound, we present in Table 2 the values of N_{mesh} required to obtain an accuracy of machine

Table 2 Number of mesh points N_{mesh} required for the Gauss–Jacobi quadrature to be applied to a range of test problems (see Appendix A). The values are predicted using (3.12), with $E_{N_{\text{mesh}}}$ set as machine epsilon eps

(a, b, z)	(1, 3, 10)	(8.1, 10.1, 100)	(1, 2, 600)	$(10^{-3}, 1, 700)$	(4, 8, 200)
N_{mesh}	15	77	429	499	148

epsilon eps for a range of test problems. We highlight that the value of a does not affect the predicted values, as this parameter does not appear in the inequality (3.12).

Gauss–Jacobi quadrature is a natural choice because of the form of the integrand in (3.11) and the fact that the integrand blows up at the end points of the integral. To implement Gauss–Jacobi quadrature, we use the Golub–Welsch algorithm [38], though of course other methods are possible (e.g., the Glaser–Liu–Rokhlin algorithm [36] or the Hale–Townsend algorithm [39]). As illustrated in Table 9, we find that using Gauss–Jacobi quadrature is effective for a large range of values of $|z|$, provided z does not have an imaginary part with magnitude greater than roughly 100. Additionally, a problem arises when either a or b becomes fairly large. A problem also occurs if $|z|$ is large, as the integral under consideration is then highly oscillatory and/or stiff.

For small values of a and b (up to about 30–40), the method of Gauss–Jacobi quadrature is extremely useful for evaluating the confluent hypergeometric function when $b > a > 0$, as the methods that we described in previous sections are not always reliable in this parameter regime. Due to the computational expense of running the algorithm, which is greater than the cost of implementing many of the series expansion methods discussed previously, we only recommend a quadrature approach in parameter regimes where series methods are likely to struggle—for example, in regimes involving large values of $|z|$.

3.6 Recurrence relations

When computing the confluent hypergeometric function, a method’s robustness—i.e., the range of parameter and variable values for which it is effective—is often greatly reduced by its poor performance as $|\text{Re}(a)|$ or $|\text{Re}(b)|$ increases. In this section, we detail recurrence-relation techniques, which can reduce the problem of computation with large parameter values to a simpler problem of computing $M(a; b; z)$ with values of $|\text{Re}(a)|$ and $|\text{Re}(b)|$ that are much closer to 0. One of the methods discussed in Sections 3.2–3.5 can subsequently be applied to solve the simpler problem, usually with much greater success than with a direct computation.

The function $M(a; b; z)$ satisfies the following recurrence relations [33, 34, 88]:

$$\begin{aligned}
 (b - a)M(a - 1; b; z) + (2a - b + z)M(a; b; z) - aM(a + 1; b; z) &= 0, \\
 b(b - 1)M(a; b - 1; z) + b(1 - b - z)M(a; b; z) + z(b - a)M(a; b + 1; z) &= 0, \\
 b(b - 1)M(a - 1; b - 1; z) - b(b - z - 1)M(a; b; z) - azM(a + 1; b + 1; z) &= 0, \quad (3.13)
 \end{aligned}$$

from which \mathbf{M} can be computed. We denote these recurrence relationships using the standard notation $(+0)$, $(0+)$, and $(++)$ [33, 88]. The $+$ indicates which parameters $(a, b, \text{ or both})$ have increasing real part. A naïve way of using these relationships is via direct application. However, for certain parameter regimes, it is instead appropriate to utilize the theory of *minimal solutions* of a recurrence relationship.

A solution f_n of a recurrence relation

$$y_{n+1} + b_n y_n + a_n y_{n-1} = 0 \tag{3.14}$$

is said to be a *minimal solution* if there exists a linearly independent solution g_n (called a *dominant solution*) such that

$$\lim_{n \rightarrow +\infty} \frac{f_n}{g_n} = 0.$$

We use the following theorem, discussed in [33, 34, 88], in our subsequent investigation of recurrence relations.

Theorem 1 (Poincaré’s Theorem) Consider the recurrence relation (3.14), where $\lim_{n \rightarrow +\infty} b_n = b_\infty$ and $\lim_{n \rightarrow +\infty} a_n = a_\infty$. Denote the zeros of the equation $t^2 + b_\infty t + a_\infty = 0$ by t_1 and t_2 . If $|t_1| \neq |t_2|$, then the recurrence relation (3.14) has two linearly independent solutions f_n, g_n such that

$$\lim_{n \rightarrow +\infty} \frac{f_n}{f_{n-1}} = t_1, \quad \lim_{n \rightarrow +\infty} \frac{g_n}{g_{n-1}} = t_2.$$

If $|t_1| = |t_2|$, then

$$\limsup_{n \rightarrow +\infty} |y_n|^{1/n} = |t_1|$$

for any nontrivial solution y_n of (3.14).

Finally, when $|t_1| \neq |t_2|$, the solution whose ratio of consecutive terms tends to the root of smaller modulus is always the minimal solution. \square

We now consider the recurrence relations (3.13), which can be modified to relations of the form (3.14), with

$$\begin{aligned} (+0) : \quad & a_n = \frac{a-b+n}{a+n}, \quad b_n = -\frac{2a-b+z+2n}{a+n}, \\ (0+) : \quad & a_n = \frac{b-a+n-1}{z}, \quad b_n = \frac{1-b-n-z}{z}, \\ (++) : \quad & a_n = -\frac{1}{(a+n)z}, \quad b_n = \frac{b-z-1+n}{(a+n)z}. \end{aligned}$$

The solutions to the recursion relations (3.15) and their ratios as $n \rightarrow +\infty$ (for real z) become [34]

$$\begin{aligned} f_n &= \Gamma(1 + a + n - b)U(a + n; b; z), \quad g_n = M(a + n; b; z), \quad \frac{f_n}{g_n} \sim e^{-4\sqrt{nz}}, \tag{3.15} \\ f_n &= \Gamma(b + n - a)\mathbf{M}(a; b + n; z), \quad g_n = U(a; b + n; z), \quad \frac{f_n}{f_{n-1}} \sim 1, \quad \frac{g_{n+1}}{g_n} \sim \frac{n}{z}, \\ f_n &= \mathbf{M}(a + n; b + n; z), \quad g_n = (-1)^n U(a + n; b + n; z), \quad \frac{f_n}{f_{n-1}} \sim \frac{1}{n}, \quad \frac{g_n}{g_{n-1}} \sim -\frac{1}{z}. \end{aligned}$$

Using (3.15), the definition of a minimal solution, and Poincaré’s Theorem, one can deduce that the minimal solutions of the relations (+0), (0+), and (++) are, respectively, $\Gamma(1+a+n-b)U(a+n; b; z)$, $\Gamma(b+n-a)\mathbf{M}(a; b+n; z)$, and $\mathbf{M}(a+n; b+n; z)$. When applying the (+0) recursion, however, the solution is only minimal in $\mathbb{C} \setminus \mathbb{R}$ [88], making this a less convenient approach in the large- $|a|$ case.

3.6.1 Miller’s algorithm

Suppose that we seek a solution of the three-term recurrence relation (3.14). One method to compute numerical approximations of \tilde{f}_n (with $n = 0, \dots, k$) for a minimal solution f_n (if the recurrence admits such a solution³) is to apply *Miller’s algorithm* [34]. The solution $\frac{f_k}{f_N}$ satisfies the following system:

$$\begin{pmatrix} a_1 & b_1 & 1 & & & & \\ & a_2 & b_2 & 1 & & & \\ & & \ddots & \ddots & \ddots & & \\ & & & a_{N-1} & b_{N-1} & 1 & \\ & & & & 1 & 0 & \\ & & & & & & 1 \end{pmatrix} \begin{pmatrix} f_0/f_N \\ f_1/f_N \\ \vdots \\ f_{N-1}/f_N \\ 1 \\ f_{N+1}/f_N \end{pmatrix} = \begin{pmatrix} 0 \\ 0 \\ \vdots \\ 0 \\ 1 \\ f_{N+1}/f_N \end{pmatrix}.$$

Miller’s algorithm involves observing that $f_{N+1}/f_N \rightarrow 0$ as $N \rightarrow \infty$. Thus, we can approximate f_k/f_N by y_k^N , which solves

$$\begin{pmatrix} a_1 & b_1 & 1 & & & & \\ & a_2 & b_2 & 1 & & & \\ & & \ddots & \ddots & \ddots & & \\ & & & a_{N-1} & b_{N-1} & 1 & \\ & & & & 1 & 0 & \\ & & & & & & 1 \end{pmatrix} \begin{pmatrix} y_0^N \\ y_1^N \\ \vdots \\ y_{N-1}^N \\ y_N^N \\ y_{N+1}^N \end{pmatrix} = \begin{pmatrix} 0 \\ 0 \\ \vdots \\ 0 \\ 1 \\ 0 \end{pmatrix}.$$

We thereby obtain the approximation $f_k \approx \frac{f_0}{y_0^N} y_k^N$. The issue is choosing N so that this approximation is within a given tolerance. The standard procedure is to continually increase N until the desired f_k has changed less than a prescribed tolerance. That is, we want to verify

$$\left| \frac{f_0}{y_0^{N+1}} y_k^{N+1} - \frac{f_0}{y_0^N} y_k^N \right| < \tau \circ 1.$$

As discussed in [34], an important consideration when applying this method in cases where y_0^N could become 0 (or when it is difficult to compute) is that of normalizing conditions. In more detail, a normalizing condition can be taken as a linear sum of minimal solutions f_n (when known); an equivalent sum can then be computed for the numerically generated functions, which are truncated appropriately

³When a minimal solution exists, it corresponds to f_n in the notation of this section.

We note that considerable research has investigated how to compute the *Whittaker function*, which is closely related to the confluent hypergeometric function. Techniques from such inquiries can perhaps be adapted for the computation of \mathbf{M} . Details of methods for computing the Whittaker function can be found in Refs. [7, 17, 50, 67, 73, 76, 78, 110].

3.8 Summary and discussion

The methods that we have examined and implemented⁴ for the computation of $\mathbf{M}(a; b; z)$ include the series methods in Sections 3.2, 3.3, and 3.4; the use of quadrature in Section 3.5; recurrence relations in Section 3.6; and various methods that are described in Section 3.7.

The series methods seemed to generate the most accurate results, and they have very fast computation times in comparison to the inbuilt MATLAB function `hypergeom`. Additionally, for values of $|a|$ and $|z|$ less than about 50 and $|b| \gtrsim 1$, the Taylor series methods described in Section 3.2 and the method of expressing ${}_1F_1$ as a single fraction in Section 3.2.1 seem typically to be sufficiently robust (with the restriction for the single-fraction method that $|b| \lesssim 1$). The method of Gauss–Jacobi quadrature is also effective for “moderate” values of $|a|$, $|b|$, and $|z|$.

One parameter regime in which the Taylor series and single-fraction methods both fail when one might expect them to succeed is when $|a|$ and $|z|$ are between roughly 10 and 60 with real parts of opposite signs (the problem arises from cancellation). In this case, the method involving Buchholz polynomials discussed in Section 3.3 can be very useful. One can do effective computations for large $|z|$ (another important case) by applying the asymptotic expansions of Section 3.4. In Section 3.4, we also mentioned hyperasymptotics, which have exponentially improved accuracy. Their use can provide a viable alternative for the computation of \mathbf{M} for large $|z|$ when software with high precision and programs to compute the incomplete gamma function in the entire complex plane are available [74, 77].

If $|\operatorname{Re}(a)| \gtrsim 50$ or $|\operatorname{Re}(b)| \gtrsim 50$, one can use the recurrence relations that we detailed in Section 3.6 to compute hypergeometric functions with parameter values that have real parts of smaller absolute value. One then completes the computation in this new parameter regime using one of the methods discussed above.

When the parameters and the variable are all real, the main problem that one faces is cancellation. For example, when computing a series representation of ${}_1F_1$ (or \mathbf{M}) in which positive and negative terms alternate, we find that the resulting error properties are likely to be poor. For instance, consider the computation of ${}_1F_1(50; 20; -100)$ or $\mathbf{M}(50; 20; -100)$. The sum of all of the positive Taylor series terms for ${}_1F_1(50; 20; -100)$ is the same as the absolute value of the sum of all of the negative terms (roughly 1.7×10^{62}) to 16 digits, whereas the value of ${}_1F_1(50; 20; -100)$ is roughly 1.4×10^{-40} . This problem can be circumvented by applying forward recurrences so that the values of b in the eventual direct computation of \mathbf{M} are (positive and) large enough that the terms cancelling each other now

⁴We have made MATLAB code available at [116].

have smaller magnitudes. We have thereby devised an effective strategy for computing \mathbf{M} for real parameters and variables. We use the result (3.2) and show our aggregate strategy in Table 3.

Extending the parameters and the variable into the complex plane makes the problem of computing the confluent hypergeometric function much more complicated. We summarize our recommendations in Fig. 4, which shows which parameter and variable values are appropriate for each of the methods that we have discussed. Details of other software for the computation of the confluent hypergeometric function are discussed in Refs. [23, 41, 53, 61, 62, 96].

4 Computation of the Gauss hypergeometric function \mathbf{F}

In this section, we discuss methods to compute the Gauss hypergeometric function $\mathbf{F}(a, b; c; z)$ accurately and quickly, and we provide recommendations for the most effective methods for each parameter and variable regime. We implement ideas of a similar nature to those that we discussed for the confluent hypergeometric function—such as those in Sections 4.2 and 4.3—and we also consider additional methods, such as specific transformations and analytic-continuation formulas, that are applicable only to \mathbf{F} . We then discuss additional methods in Section 4.7 and summarize our proposed computational strategy in Section 4.8.

Table 3 Recommendations for which methods to use for computing the confluent hypergeometric function when the parameters and the variable are real

Case	Regions for a, b, z	Recommended method(s)	Relevant sections and references
I(A)	$a, b \geq 0, z \geq 0$	Taylor series methods; Single-fraction method; Buchholz polynomial method; (Hyper)asymptotics; Gauss–Jacobi quadrature, if $b > a > 0$;	3.2 [3, 63] 3.2.1 [64, 65] 3.3 [1, 2] 3.4 [3, 9, 68, 72, 74, 77] 3.5 [26]
I(B)	$a, b \geq 0, z < 0$	Forward recursion to combat cancellation, then Taylor series or single-fraction method	3.6 [34, 88] 3.2 [3, 63] 3.2.1 [64, 65]
II	$a < 0, b \geq 0$	Transformation (3.2), then same as for case I	3.8 [110, Eq. (13.2.39)]
III	$a, b < 0$	Forward recursion to combat cancellation, then Taylor series or single-fraction method	3.6 [34, 88] 3.2 [3, 63] 3.2.1 [64, 65]
IV	$a \geq 0, b < 0$	Recurrence relations; Transformation (3.2), then same as for case III	3.6 [34, 88] 3.8 [110, Eq. (13.2.39)]

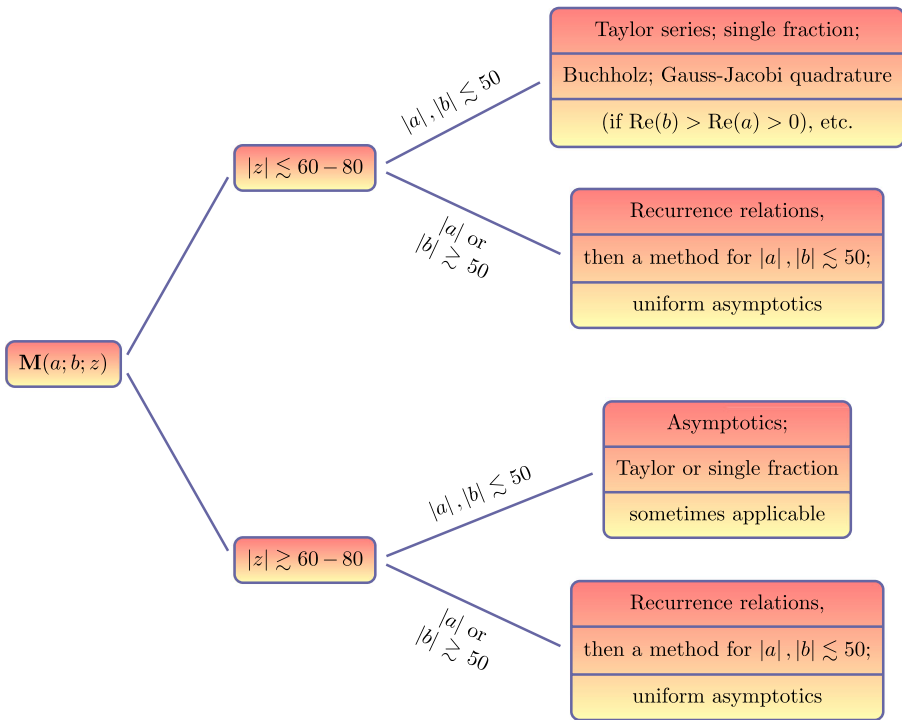


Fig. 4 Summary of recommended methods for computing \mathbf{M} for different regions of a, b , and z . (The “etc.” in the upper right signifies that one can also use other methods from Section 3.7)

4.1 Properties of \mathbf{F}

As we indicated in Section 2, the *Gauss hypergeometric function* $\mathbf{F}(a, b; c; z)$ is defined as the series (2.2) when z is in the radius of convergence (i.e., when $|z| < 1$). This series is defined for any $a \in \mathbb{C}, b \in \mathbb{C}$, and $c \in \mathbb{C}$. For z outside this range, $\mathbf{F}(a, b; c; z)$ is defined by analytic continuation, which we detail in Section 4.5. This makes it possible to consider the computation of \mathbf{F} for any $z \in \mathbb{C}$.

Note that $\mathbf{F}(a, b; c; 0) = \frac{1}{\Gamma(c)}$ for any $a, b \in \mathbb{C}$ and $c \notin \mathbb{Z}^- \cup \{0\}$. If $c = n \in \mathbb{Z}^- \cup \{0\}$, then (2.2) is given by a polynomial in z of degree $-n$. On the unit disk $|z| = 1$, the series in (2.2) converges absolutely when $\text{Re}(c - a - b) > 0$ [3], and it attains the value $\frac{\Gamma(c-a-b)}{\Gamma(c-a)\Gamma(c-b)}$ at $z = 1$ [84]. The series converges conditionally for $-1 < \text{Re}(c - a - b) \leq 0$ (except at $z = 1$), and it does not converge for $\text{Re}(c - a - b) \leq -1$ [3].

The Gauss hypergeometric function also satisfies the differential equation (2.5). When $c \in \mathbb{Z}^- \cup \{0\}$, one uses the fact that the function $\mathbf{F}(a, b; c; z) = \sum_{j=0}^{\infty} \frac{(a)_j (b)_j}{\Gamma(c+j)} \frac{z^j}{j!}$ is a solution for $|z| < 1$ and any $c \in \mathbb{C}$. Most methods that we describe can be modified to compute ${}_2F_1(a, b; c; z)$ as well. The differential equation (2.5) has three singular points: $z = 0, z = 1$, and $z = \infty$.

As discussed in Ref. [73], one constructs a branch cut between $z = 1$ and $z = +\infty$. The branch in the sector $|\arg(1 - z)| < \pi$ is considered to be the principle branch, and we aim to compute F in this branch.

As was the case with the confluent hypergeometric function, the Gauss hypergeometric function arises in a wide range of applications. For instance, F can be used to describe transonic adiabatic flow over a smooth bump in an ideal compressible fluid [13]. It has also appeared in investigations of a plasma dispersion function [59], penetration by electrons of a potential barrier [18], the density of infected nodes in the susceptible–infected–susceptible (SIS) epidemic model on networks [79], scintillation indices of beams [19, 48], stochastic dynamical systems [103], electroosmosis of non-Newtonian fluids [109], and more.

4.2 Taylor series

In this section, we carry out computations of the Gauss hypergeometric function using its Taylor series representation (2.2) and discuss the accuracy of these computations for different parameter and variable regimes.

As with the confluent hypergeometric function in Section 3.2, we use two methods to compute the series

$${}_2F_1(a, b; c; z) = \sum_{j=0}^{\infty} \underbrace{\frac{(a)_j (b)_j}{(c)_j}}_{C_j} \frac{1}{j!} z^j. \tag{4.1}$$

Method (a) We compute

$$C_0 = 1, \quad S_0 = C_0, \\ C_{j+1} = C_j \frac{(a + j)(b + j)}{c + j} \frac{z}{j + 1}, \quad S_{j+1} = S_j + C_{j+1}, \quad j = 0, 1, 2, \dots,$$

where C_j denotes the $(j + 1)$ th term of the Taylor series (2.2) and S_j denotes the sum of the first $j + 1$ terms.

We stop the summation either when $\frac{|C_{N+1}|}{|S_N|} < \text{tol}$ for some tol and some N or when two successive terms are small compared to S_N . We then return S_N as the solution.

Method (b) As with the recommended method of Ref. [63] for computing ${}_1F_1$ that we discussed in Section 3.2, one can compute a recurrence relation for an approximation of the Gauss hypergeometric function in terms of the two previous approximations in an iterative scheme:

$$S_{-1} = S_0 = 1, \quad S_1 = 1 + \frac{ab}{c} z, \\ r_j = \frac{(a + j - 1)(b + j - 1)}{j(c + j - 1)}, \quad S_j = S_{j-1} + (S_{j-1} - S_{j-2})r_j z, \quad j = 2, 3, \dots$$

We stop the summation either when $\frac{|S_{N+1}-S_N|}{|S_N|} < \text{tol}$ for some tol and some N or when two or more successive terms are small. We then return S_N as the solution. For our numerical tests, we use the second of these stopping criteria.

Methods (a) and (b) both amount to truncating the series

$$S_\infty = \sum_{j=0}^\infty \frac{(a)_j (b)_j}{(c)_j} \frac{z^j}{j!}. \tag{4.2}$$

By using one of these two methods to compute $F(a, b; c; z)$, we can subsequently compute $\mathbf{F}(a, b; c; z)$ using the expression $F(a, b; c; z) = \Gamma(c)\mathbf{F}(a, b; c; z)$. The exception to this is when $c \in \mathbb{Z}^- \cup \{0\}$, in which case more care must be taken (which we saw is also the case for the confluent hypergeometric function).

As shown in Table 10, Methods (a) and (b) have similar levels of effectiveness in terms of accuracy and number of terms required for computation. Both methods work very successfully when the parameter values have small magnitudes (especially when $|a|, |b|, |c| \leq 20$), and the time that it takes for the computation is significantly shorter than that taken by the inbuilt MATLAB program. Furthermore, when c is relatively large in magnitude compared to a, b , and z , we observe excellent convergence properties for both Taylor series methods, as (4.1) can be viewed as an asymptotic expansion in this parameter regime. However, computing \mathbf{F} (before the stopping criterion is met) with Taylor series requires more terms than was the case for computing \mathbf{M} . In Fig. 5, we show the number of points required for the computation of three test cases with real $z \in [-1, 1]$. As one can see, this illustrates that many more points are required for the computation as z approaches the unit circle.

We can compute ${}_2F_1$ very accurately for a range of cases with large real parameter values (with $c < a < 0$ and $c < b < 0$). However, the Taylor series methods are much less effective when either $|a|$ or $|b|$ is much greater than $|c|$. For such cases,

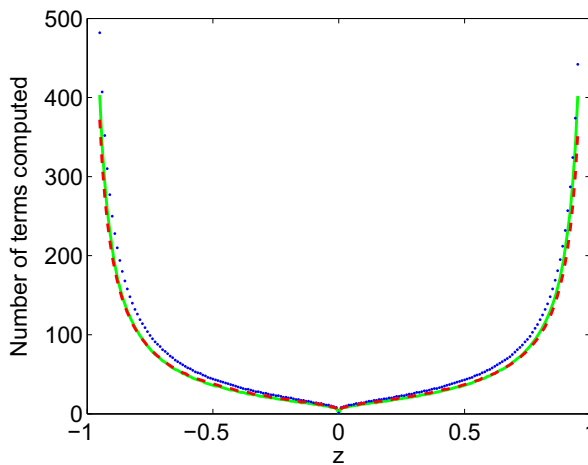


Fig. 5 (Color online) Number of terms that need to be computed using the Taylor series Method (a) for evaluating ${}_2F_1$ (and hence \mathbf{F}) for real $z \in [-0.95, 0.95]$ when $a = 1.5, b = 1 + 2i, c = 4.5 + 5i$ (red, dashed), $a = 0.15, b = 0.2, c = 1.1$ (green, solid), and $a = 3, b = 2, c = 6.5$ (blue, dotted) before the stopping criterion (two successive small terms) is satisfied. The method gives results to 14-digit accuracy

one should employ the recurrence relations that we will discuss in Section 4.6.1. We conclude that the region in which the Taylor series methods seem to be effective is $|z| \lesssim 0.9$, provided the values of a , b , and c do not result in cancellation.

Other series expressions for ${}_2F_1$ are also available. For example, Ref. [82] discussed an expansion in terms of $\widehat{z} := \frac{\sqrt{1-z}-1}{\sqrt{1-z}+1}$. This expansion converges for $|\widehat{z}| < 1$, which is a less restrictive condition than the convergence criterion for (4.1).

4.2.1 Writing the Gauss hypergeometric function as a single fraction

As with the confluent hypergeometric function, we can compute the Gauss hypergeometric function by representing it as a single fraction. We now examine the accuracy and robustness of this approach and indicate parameter regimes for which it is particularly effective.

Method (c) As we discussed for the confluent hypergeometric function in Section 3.2.1, one can express ${}_2F_1(a, b; c; z)$ as a single fraction using recurrence relations. One starts with $\alpha_0 = 0$, $\beta_0 = 1$, $\gamma_0 = 1$, and $S_0 = 1$, and the recurrence relation is given by

$$\begin{aligned} \alpha_j &= (\alpha_{j-1} + \beta_{j-1})j(c + j - 1), \\ \beta_j &= \beta_{j-1}(a + j - 1)(b + j - 1)z, \\ \gamma_j &= \gamma_{j-1}j(c + j - 1), \\ S_j &= \frac{\alpha_j + \beta_j}{\gamma_j}, \quad j = 1, 2, \dots \end{aligned} \tag{4.3}$$

This generates a sequence of approximations S_j (with $j = 1, 2, \dots$) to ${}_2F_1(a, b; c; z)$. We can select stopping criteria in the same way as for the other Taylor series methods discussed above.

As indicated in Table 10, this approach works well for small values of the parameters and variable. (As a rough guide, it is good for $|a|, |b|, |c| \lesssim 20$, and $|z| \lesssim 0.9$.) In particular, this method becomes more successful for computing \mathbf{F} as $|c|$ becomes smaller or c becomes closer to an integer. The reason is the same as it is for the analogous method for confluent hypergeometric functions when computing \mathbf{M} for small $|b|$, and this issue is also relevant when b is close to $-m$, where $m \in \mathbb{Z}^+ \cup \{0\}$.

However, this method does struggle more than the Taylor series methods when either a or b has large magnitude (greater than roughly 50) due to a greater risk of overflow—i.e., the program is attempting to compute values that are larger than it can handle—from the potentially large numerators and denominators in (4.3). For such cases, a sensible approach is to divide α_j , β_j , and γ_j by the same quantity at regular intervals. Alternatively, one can use other methods, such as the recurrence relations that we will describe in Section 4.6.1.

4.3 Quadrature methods

In Section 3.5, we discussed quadrature methods for computing $\mathbf{M}(a; b; z)$. We now apply the method of Gauss–Jacobi quadrature to compute $\mathbf{F}(a, b; c; z)$ for real b and c when $c > b > 0$ and $|\arg(1 - z)| < \pi$. In this parameter and variable regime, the

function $\mathbf{F}(a, b; c; z)$ has the integral representation [3]

$$\mathbf{F}(a, b; c; z) = \frac{1}{\Gamma(b)\Gamma(c-b)} \int_0^1 (1-zt)^{-a} (1-t)^{c-b-1} t^{b-1} dt. \tag{4.4}$$

Note that a and b can be interchanged in the series definition (2.2) of ${}_2F_1$, so we can also apply equation (4.4) to $\mathbf{F}(b, a; c; z)$ if $c > a > 0$ (and a is real).⁵

Transforming $t \mapsto \frac{1}{2}\tilde{t} + \frac{1}{2}$ and defining the Jacobi parameters $\tilde{\alpha} = c - b - 1$ and $\tilde{\beta} = b - 1$ yields [26]

$$\begin{aligned} \mathbf{F}(a, b; c; z) &= \frac{1}{2^{c-1}\Gamma(b)\Gamma(c-b)} \int_{-1}^1 \left(\left(1 - \frac{z}{2}\right) - \frac{1}{2}z\tilde{t} \right)^{-a} (1-\tilde{t})^{c-b-1} (1+\tilde{t})^{b-1} d\tilde{t} \\ &= \frac{1}{\Gamma(b)\Gamma(c-b)} \left[\sum_{j=1}^{N_{\text{mesh}}} w_j^{GJ} \left(\left(1 - \frac{z}{2}\right) - \frac{1}{2}z t_j^{GJ} \right)^{-a} + E_{N_{\text{mesh}}}(a; b; z) \right], \end{aligned}$$

where t_j^{GJ} and w_j^{GJ} are (respectively) the Gauss–Jacobi nodes and weights on $[-1, 1]$ and N_{mesh} is the number of mesh points. Error bounds for this method are discussed in Ref. [26].

If a is real and $c > a > 0$, then switching the parameters a and b in the definition of $\mathbf{F}(a, b; c; z)$ allows one to apply the method of Gauss–Jacobi quadrature. As with \mathbf{M} , the integrand in (4.4) blows up at the end points of the integral. This motivates the choice of Gauss–Jacobi quadrature to perform the required integration numerically.

The results in Table 10 illustrate that applying Gauss–Jacobi quadrature to the integral in (4.4) is a useful method for computing the Gauss hypergeometric function when $c > b > 0$. If the moduli of the parameters a, b , and c are at least 50–100, then Gauss–Jacobi quadrature often performs better than Taylor series approaches. The method also works well near the points $z = e^{\pm i\pi/3}$, which are notoriously difficult to compute (see the discussions in Sections 4.4 and 4.5), especially for smaller values of $|a|$ and $|b|$.

Therefore, as with ${}_1F_1$ (see Section 3.5), applying Gauss–Jacobi quadrature to compute ${}_2F_1$ is potentially a useful method when the parameters a, b , and c have moduli that are not too large. However, due to the relatively high computational cost of running this algorithm in comparison to many of the series expansion methods previously outlined, we only recommend this approach for parameter regimes in which a series method is likely to generate inaccurate solutions.

4.4 Computing \mathbf{F} for z near or outside the unit disk

The methods that we have discussed thus far are generally very useful for computing \mathbf{F} for $|z| \lesssim 0.9$. In this section, we discuss how to use these computations to compute \mathbf{F} effectively for any $z \in \mathbb{C}$. This can be done either by applying transformation

⁵The integral representation (4.4) is valid in the more general parameter regime $\text{Re}(c) > \text{Re}(b) > 0$; however, Gauss–Jacobi quadrature can only be applied for real b and c .

Table 4 List of transformations of $z \in \mathbb{R}$ [23] for which $0 \leq w \leq \rho = \frac{1}{2}$

Case	Interval	Transformation
1	$-\infty < z < -1$	$w = \frac{1}{1-z}$
2	$-1 \leq z < 0$	$w = \frac{z}{z-1}$
3	$0 \leq z \leq \frac{1}{2}$	$w = z$
4	$\frac{1}{2} < z \leq 1$	$w = 1 - z$
5	$1 < z \leq 2$	$w = 1 - \frac{1}{z}$
6	$2 < z < \infty$	$w = \frac{1}{z}$

formulas to the results from previous sections or by using expansions derived for the special cases $b - a \in \mathbb{Z}$ and $c - a - b \in \mathbb{Z}$.

4.4.1 Transformation formulas

Because the series (2.2) converges only for $|z| < 1$, and because it converges more rapidly as $|z|$ becomes smaller, it is important to use transformation formulas that reduce the problem of computing (2.2) for a value of $|z|$ near or greater than 1 to a problem of computing the series for a new variable w with a much smaller magnitude. We describe such transformation formulas in this section.

The idea of these transformations is to map as large a region of the complex plane as possible onto disks $|w| \leq \rho$ for a number $\rho \in (0, 1]$ that is as close to 0 as possible. This is desirable because the function \mathbf{F} can be computed faster and more accurately when $|z|$ is near 0. Finding representations of \mathbf{F} that make it possible to carry out the computation in terms of the new variable w allows one to obtain more accurate results than by using the methods that we described previously. We show such transformation formulas for real z in Table 4. These transformations map any $z \in \mathbb{R}$ to a new variable $w \in [0, \frac{1}{2}]$.

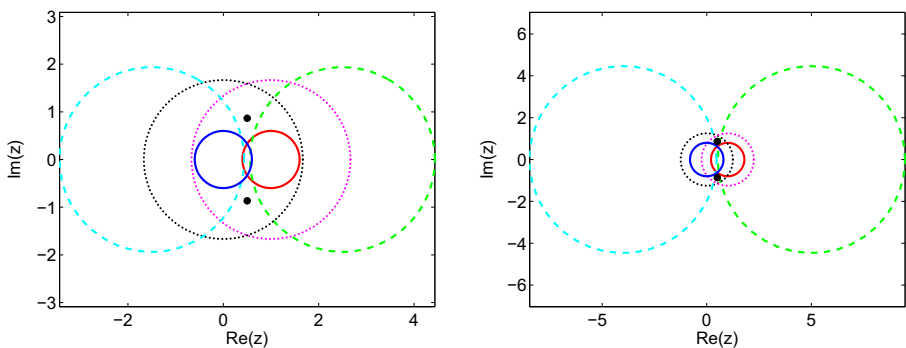


Fig. 6 (Color online) The curves $|z| = \rho$ (dark blue, solid, left inner), $|\frac{1}{z}| = \rho$ (black, dotted, left middle), $|1 - z| = \rho$ (red, solid, right inner), $|\frac{1}{1-z}| = \rho$ (purple, dotted, right middle), $|\frac{z}{z-1}| = \rho$ (sky blue, dashed, left outer), and $|1 - \frac{1}{z}| = \rho$ (green, dashed, right outer) for (left panel) $\rho = 0.6$ and (right panel) $\rho = 0.8$. We show the points $z = e^{\pm i\pi/3}$ using black dots. (These figures are adapted from plots in Refs. [28, 34])

For complex z , the problem is more complicated. In Fig. 6, we show plots of $|w| = \rho$ for each of the six expressions for w given in Table 4 for $\rho = 0.6$ and $\rho = 0.8$. If one wishes to apply one of the six transformations in Table 4, it is necessary that $|w| \leq \rho$ is satisfied for at least one representation of w in the table. The region in Fig. 6 in which none of the representations of w satisfy $|w| \leq \rho$ either surrounds or is near the points $z = e^{\pm i\pi/3} = \frac{1}{2}(1 \pm i\sqrt{3})$ (which are marked as dots). As ρ increases towards the value 1, the region in which none of the transformations satisfy $|w| \leq \rho$ becomes smaller, but it remains near the points $z = e^{\pm i\pi/3}$ because the set $\{e^{i\pi/3}, e^{-i\pi/3}\}$ is mapped to itself by each of the six transformations in Table 4. We discuss the case $z \approx e^{\pm i\pi/3}$ in more detail in Section 4.5 and noted it briefly in Section 4.3. The five transformations that are useful when $z \not\approx e^{\pm i\pi/3}$ are [3, 20, 23, 108]

$$\begin{aligned} \frac{\sin(\pi[b-a])}{\pi} \mathbf{F}(a, b; c; z) &= \frac{(1-z)^{-a}}{\Gamma(b)\Gamma(c-a)} \mathbf{F}\left(a, c-b; a-b+1; \frac{1}{1-z}\right) \\ &\quad - \frac{(1-z)^{-b}}{\Gamma(a)\Gamma(c-b)} \mathbf{F}\left(b, c-a; b-a+1; \frac{1}{1-z}\right), \end{aligned} \tag{4.5}$$

$$\mathbf{F}(a, b; c; z) = (1-z)^{-a} \mathbf{F}\left(a, c-b; c; \frac{z}{z-1}\right), \tag{4.6}$$

$$\begin{aligned} \frac{\sin(\pi[c-a-b])}{\pi} \mathbf{F}(a, b; c; z) &= \frac{1}{\Gamma(c-a)\Gamma(c-b)} \mathbf{F}(a, b; a+b-c+1; 1-z) \\ &\quad - \frac{(1-z)^{c-a-b}}{\Gamma(a)\Gamma(b)} \mathbf{F}(c-a, c-b; c-a-b+1; 1-z), \end{aligned} \tag{4.7}$$

$$\begin{aligned} \frac{\sin(\pi[c-a-b])}{\pi} \mathbf{F}(a, b; c; z) &= \frac{z^{-a}}{\Gamma(c-a)\Gamma(c-b)} \mathbf{F}\left(a, a-c+1; a+b-c+1; 1-\frac{1}{z}\right) \\ &\quad - \frac{z^{a-c}(1-z)^{c-a-b}}{\Gamma(a)\Gamma(b)} \mathbf{F}\left(c-a, 1-a; c-a-b+1; 1-\frac{1}{z}\right), \end{aligned} \tag{4.8}$$

$$\begin{aligned} \frac{\sin(\pi[b-a])}{\pi} \mathbf{F}(a, b; c; z) &= \frac{(-z)^{-a}}{\Gamma(b)\Gamma(c-a)} \mathbf{F}\left(a, a-c+1; a-b+1; \frac{1}{z}\right) \\ &\quad - \frac{(-z)^{-b}}{\Gamma(a)\Gamma(c-b)} \mathbf{F}\left(b-c+1, b; b-a+1; \frac{1}{z}\right), \end{aligned} \tag{4.9}$$

where formulas (4.6)–(4.8) require that $|\arg(1-z)| < \pi$, formulas (4.7)–(4.8) additionally require that $|\arg z| < \pi$, and formulas (4.5) and (4.9) require that $|\arg(-z)| < \pi$.

We tested formulas (4.5)–(4.9) on a large range of parameter and variable values and found that they successfully compute \mathbf{F} for variable values close to the unit disk or with modulus greater than 1 in terms of new variables with smaller magnitude, provided z is not too close to $e^{\pm i\pi/3}$. However, due to the presence of $\Gamma(a-b)$, $\Gamma(b-a)$, $\Gamma(c-a-b)$, and $\Gamma(a+b-c)$ factors in (4.5)–(4.9), the cases $b-a \in \mathbb{Z}$ and $c-a-b \in \mathbb{Z}$ cannot be handled by applying the transformations in Table 4, when computing ${}_2F_1$. There are also numerical issues when either $b-a$ or $c-a-b$ is close to an integer, as two large conflicting terms are being added together (leading to cancellation).

4.4.2 Cases $b-a \in \mathbb{Z}$ and $c-a-b \in \mathbb{Z}$

References [3, 20] discussed formulas that avoid the above cancellation issue when either $b-a$ or $c-a-b$ is exactly equal to an integer. These cases can be computed

using the ideas detailed in Section 3.2. Reference [23] derived expressions for $b - a$ or $c - a - b$ close to an integer using a polynomial expansion for the Gamma function. Reference [61] showed how to exploit the Lanczos expansion and other properties of the Gamma function for successful computation when $b - a$ or $c - a - b$ is close to an integer.

4.5 Analytic-continuation formulas for $z \approx e^{\pm i\pi/3}$

Applying the transformation formulas of Section 4.4 becomes a much less viable method as z approaches the points $z = e^{\pm i\pi/3} = \frac{1}{2}(1 \pm i\sqrt{3})$. The reason is as follows: whatever value $\rho \in (0, 1]$ is taken for $|z| \leq \rho$, it is not possible to map the points $z = e^{\pm i\pi/3}$ onto a w in a disk of radius less than 1, as points are mapped to themselves or each other under any of the six transformations in Table 4. As ρ increases towards 1, an increasingly large number of points close to $z = e^{\pm i\pi/3}$ are mapped into such a disk, but the points themselves can never be mapped into a disk, and points very close to them require a computation that involves a prohibitively large value of ρ (for which the methods discussed thus far do not generate an accurate result).

To resolve this issue, Refs. [11, 12] gave an expansion in the form of a *continuation formula*:

$$\mathbf{F}(a, b; c; z) = \frac{\Gamma(b - a)}{\Gamma(b)\Gamma(c - a)}(z_0 - z)^{-a} \sum_{j=0}^{\infty} d_j(a, z_0)(z - z_0)^{-j} \quad (4.10)$$

$$+ \frac{\Gamma(a - b)}{\Gamma(a)\Gamma(c - b)}(z_0 - z)^{-b} \sum_{j=0}^{\infty} d_j(b, z_0)(z - z_0)^{-j},$$

where $|\arg(z_0 - z)| < \pi$, the difference $b - a$ is not an integer, and d_j is defined by

$$d_{-1}(v, z_0) = 0, d_0(v, z_0) = 1, \quad (4.11)$$

$$d_j(v, z_0) = \frac{j + v - 1}{j(j + 2v - a - b)} \left[\{(j + v)(1 - 2z_0) + (a + b + 1)z_0 - c\}d_{j-1}(v, z_0) \right. \\ \left. + z_0(1 - z_0)(j + v - 2)d_{j-2}(v, z_0) \right], j = 1, 2, \dots$$

The series in (4.10) converges at every point outside the disk $|z - z_0| = \max\{|z_0|, |z_0 - 1|\}$, so one must choose an appropriate z_0 to implement this method. The case noted in Ref. [11] is $z_0 = \frac{1}{2}$, which results in convergence outside the disk $|z - \frac{1}{2}| = \frac{1}{2}$ and, in particular, includes points close to $e^{\pm i\pi/3}$. For further details about this method, see Refs. [11, 12, 45].

For $b - a \in \mathbb{Z}$, the expansion (4.10) is not valid, as one of the Gamma functions in the numerators of the two terms in (4.10) is infinitely large. Reference [11] discussed

these issues and includes an alternative expression for $b - a = 0$. Reference [57] used a limiting process for $b - a \in \mathbb{Z} \setminus \{0\}$.

The results in Table 10 suggest that using the expansion in (4.10) is very accurate in a region that troubled the methods from Sections 4.2–4.4. Using the continuation formula (4.10) is effective not only when z is equal or close to $e^{\pm i\pi/3}$ but also when z lies outside the unit disk. However, it is ineffective when $|a| \gtrsim 30$, $|b| \gtrsim 30$, or $|c| \gtrsim 70$, although this problem can be resolved by applying recurrence relations from Section 4.6.1.

Reference [61] presented an alternative method to that suggested in Ref. [11] for computing ${}_2F_1(a, b; c; z)$ near the points $z = e^{\pm i\pi/3}$. The idea is again to expand about a point z_0 at which the expansion can be computed more easily, but this time one uses a Taylor expansion about this point in conjunction with the recurrence relation corresponding to the hypergeometric differential equation (2.5). The expansion that was obtained in Ref. [61] is

$${}_2F_1(a, b; c; z) = \sum_{n=0}^{\infty} q_n(z - z_0)^n,$$

where

$$q_0 = {}_2F_1(a, b; c; z_0), \quad q_1 = \frac{d}{dz_0} [{}_2F_1(a, b; c; z_0)] = \frac{ab}{c} {}_2F_1(a + 1, b + 1; c + 1; z_0),$$

$$q_{n+2} = \frac{1}{z_0(1 - z_0)(n + 2)} \left[\left(n(2z_0 - 1) - c + (a + b + 1)z_0 \right) q_{n+1} + \frac{(a + n)(b + n)}{n + 1} q_n \right],$$

for $n = 0, 1, 2, \dots$. One can also use these relations to compute the function $\mathbf{F}(a, b; c; z)$. The quantities q_0 and q_1 should be calculated using a method appropriate for the parameter regimes in question. As in Ref. [61], we take

$$z_0 = r_0 \frac{z}{|z|}, \quad r_0 = \begin{cases} 0.9, & \text{if } |z| \leq 1, \\ 1.1, & \text{if } |z| > 1. \end{cases}$$

The method is more convenient than the one in Ref. [11] because there are no Gamma functions in the above expression for ${}_2F_1$, so no singularities arise when $b - a \in \mathbb{Z}$ or $c - a - b \in \mathbb{Z}$. As discussed in Ref. [61], this method gives better accuracy for large $|a|$ and $|b|$. However, the method can be slow computationally due to the work of computing q_0 and q_1 .

4.6 Techniques for large values of the parameters $|a|$, $|b|$, and $|c|$

In this section, we detail two widely researched techniques that can be useful for evaluating \mathbf{F} when $|a|$, $|b|$, and $|c|$ are sufficiently large that the function cannot be evaluated effectively using methods that we described previously. The two methods that we now discuss entail the use of recurrence relations—involving computing \mathbf{F} for “nicer” parameter values and applying the recurrence relations to obtain a solution for more awkward values—or uniform asymptotics, which involves computing series for \mathbf{F} in terms of other special functions.

4.6.1 Recurrence relations

As we discussed for the confluent hypergeometric function in Section 3.6, we aim to overcome the lack of accuracy from attempting to compute the Gauss hypergeometric function for large values of $|\operatorname{Re}(a)|$, $|\operatorname{Re}(b)|$, and $|\operatorname{Re}(c)|$ or (see Section 4.8) which can sometimes occur when $|\operatorname{Re}(c)|$ is too small. We explain how this problem can be addressed using recurrence relations. We then reformulate the computation as one involving values of $|\operatorname{Re}(a)|$, $|\operatorname{Re}(b)|$, and $|\operatorname{Re}(c)|$ that are closer to 0, and then we can compute the Gauss hypergeometric function accurately using the methods discussed previously.

Recurrence relations involving the Gauss hypergeometric function $\mathbf{F}(a, b; c; z)$ are discussed in Refs. [22, 28, 33, 43, 93]. The four recurrence relations that we discuss in the present paper are described in Ref. [28]. Following the usual notation in the literature, we denote them by $(+ + 0)$, $(00+)$, $(+ + -)$, and $(+0-)$. We state them in Appendix D.

As in Section 3.6 for \mathbf{M} , we seek minimal solutions of the recurrence relations. Unlike for \mathbf{M} , however, the four recurrence relations for \mathbf{F} have different minimal

Table 5 Minimal solutions of the four recurrence relations for \mathbf{F} for z in different regions of the complex plane. See the discussion in Ref. [33]

Relation and valid region of \mathbb{C}	Minimal solution
$(+ + 0), \mathbb{C} \setminus \{z \leq 0\}$	$\Gamma(1+a-c+n)\Gamma(1+b-c+n)\mathbf{F}(a+n, b+n; 1+a+b-c+2n; 1-z)$
$(00+), \operatorname{Re}(z) < \frac{1}{2}$	$\Gamma(c+n)\mathbf{F}(a, b; c+n; z)$
$(00+), \operatorname{Re}(z) > \frac{1}{2}$	$\left(\frac{z-1}{z}\right)^n \Gamma(c+n)\mathbf{F}(1-a, 1-b; 1-a-b+c+n; 1-z)$
$(+ + -)$ Inside curve in Fig. 7 (left)	$\left(\frac{z}{z-1}\right)^n \frac{\Gamma(b-c+1+2n)\Gamma(a-c+1+2n)}{\Gamma(a+n)\Gamma(b+n)\Gamma(1-c+n)} \mathbf{F}(1-a-n, 1-b-n; 2-c+n; z)$
$(+ + -)$ Outside curve in Fig. 7 (left)	$\frac{\Gamma(b-c+1+2n)\Gamma(a-c+1+2n)}{\Gamma(1-c+n)} \mathbf{F}(a+n, b+n; 1+a+b-c+3n; 1-z)$
$(+0-)$ Inside inner curve in Fig. 7 (right)	$\left(\frac{-z}{(1-z)^2}\right)^n \frac{\Gamma(b-c+1+n)\Gamma(a-c+1+2n)}{\Gamma(a+n)\Gamma(1-c+n)} \mathbf{F}(1-a-n, 1-b; 2-c+n; z)$
$(+0-)$ Between curves in Fig. 7 (right)	$\frac{\Gamma(b-c+1+n)\Gamma(a-c+1+2n)}{\Gamma(1-c+n)} \mathbf{F}(a+n, b; 1+a+b-c+2n; 1-z)$
$(+0-)$ Outside curves in Fig. 7 (right)	$\left(\frac{-z}{(1-z)^2}\right)^n \frac{\Gamma(1+a-c+2n)}{\Gamma(1-c+n)} \mathbf{F}(1-b, -b+c-n; 1+a-b+n; \frac{1}{z})$

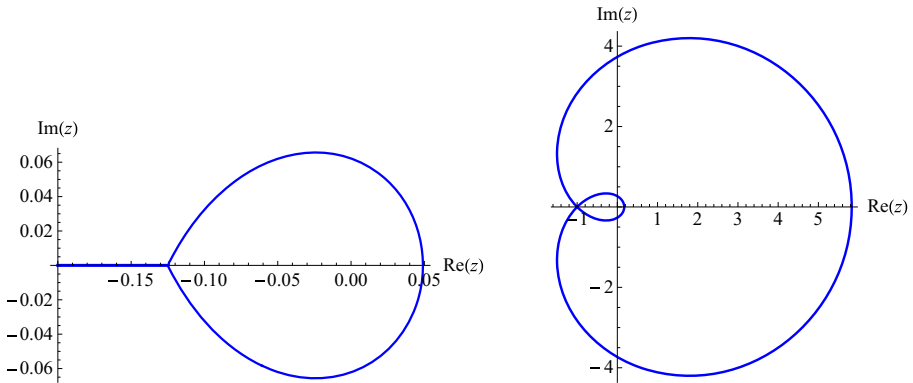


Fig. 7 Relevant regions for minimal solutions of recurrence relations (*left*) (+ + −) and (*right*) (+0−). With reference to Table 5, in the *left plot*, “Inside curve” refers to the enclosed region and “Outside curve” refers to the remainder of \mathbb{C} ; in the *right plot*, “Inside inner curve” refers to the smaller enclosed region, “Between curves” refers to the larger enclosed region, and “Outside curves” refers to the remainder of \mathbb{C}

solutions in different regions of the complex plane. We give the minimal solutions as $n \rightarrow +\infty$ for each of the four recurrence relations [33] in Table 5.

Therefore, as with \mathbf{M} in Section 3.6, we apply two different methods. First, we take the minimal solutions of the four recurrence relations in specific regions and apply the recurrence relations backwards. Second, we use the minimal solutions of the recurrence relations to apply the recurrence relations using Miller’s algorithm or Olver’s algorithm. A viable way of computing a hypergeometric function with parameters whose real parts have large moduli is therefore to compute two hypergeometric functions whose real parts have smaller moduli and then apply appropriate recurrence relations.

4.6.2 Uniform asymptotic expansions

Another potentially viable method for dealing with large values of the parameters $|a|$, $|b|$, and $|c|$ when computing $\mathbf{F}(a, b; c; z)$ is to exploit uniform asymptotic expansions. In particular, the following three uniform asymptotic expansions are useful:

- **Expansion for $\mathbf{F}(a + \lambda, b - \lambda; c; \frac{1}{2} - \frac{1}{2}z)$ as $\lambda \rightarrow \infty$ [44]:** For fixed $a, b, c \in \mathbb{C}$ and $|\arg z| < \pi$ [44] (see also [16]),

$$\mathbf{F}\left(a + \lambda, b - \lambda; c; \frac{1}{2} - \frac{1}{2}z\right) \sim 2^{\frac{1}{2}(a+b-1)}(z - 1)^{-\frac{1}{2}c}(z + 1)^{\frac{1}{2}(c-a-b-1)} \times \left(\frac{\sinh \xi}{\xi}\right)^{1/2} \sum_{m=0}^{\infty} C_m(\xi) \xi \frac{I_{c-1+m}(\alpha \xi)}{\alpha^{m+c-1}},$$

as $|\lambda| \rightarrow \infty$, where $I_\nu(z) = i^{-\nu} J_\nu(iz)$ and $J_\nu(z)$ is the Bessel function (see Appendix C). Additionally, $z = \cosh \zeta$, $\alpha = \frac{1}{2}(a - b) + \lambda$, and $C_j(\zeta)$ is defined by $C_0(\zeta) = 1$ and

$$C''_m(\zeta) + \{1 - 2(\nu + m)\} \frac{C'_m(\zeta)}{\zeta} + \{m(m + 2\nu)\} \frac{C_m(\zeta)}{\zeta^2} + 2C'_{m+1}(\zeta) = \psi(\zeta)C_m(\zeta),$$

where $m = 0, 1, 2, \dots$, the parameter $\nu = c - 1$, and

$$\psi(\zeta) = \left(\frac{3}{4} + 4c_1\right) \left(\frac{1}{\sinh^2 \zeta} - \frac{1}{\zeta^2}\right) + \frac{c_1 - \frac{1}{2}c_3}{\cosh^2 \frac{1}{2}\zeta},$$

$$c_1 = \frac{1}{4} \left\{ (c - 1)^2 - 1 \right\}, \quad c_3 = \frac{1}{2} \left\{ (a + b - c)^2 - 1 \right\}.$$

- **Expansion for ${}_2F_1(a, b - \lambda; c + \lambda; -z)$ as $\lambda \rightarrow \infty$ [69]:** For fixed $a, b, c \in \mathbb{C}$ and $|\arg z| < \pi$,

$${}_2F_1(a, b - \lambda; c + \lambda; -z) \sim \frac{2^\lambda (1+z)^{\lambda-a} \Gamma(c+\lambda) \Gamma(1-b+\lambda)}{z^{\lambda/2} \Gamma(c-b+2\lambda) \sqrt{2\pi}} \times \left(\lambda^{\frac{1}{2}(a-1)} U\left(a - \frac{1}{2}, -\alpha\sqrt{\lambda}\right) \sum_{s=0}^\infty \frac{\gamma_{0,s}}{\lambda^s} + \lambda^{\frac{1}{2}(a-2)} U\left(a - \frac{3}{2}, -\alpha\sqrt{\lambda}\right) \sum_{s=0}^\infty \frac{\gamma_{1,s}}{\lambda^s} \right),$$

as $\lambda \rightarrow \infty$ in $|\arg \lambda| \leq \pi - \delta < \pi$, where $U(a, z)$ is the parabolic cylinder function (see Appendix C). Additionally, $\frac{1}{2}\alpha^2 = -\ln\left(\frac{4z}{(z+1)^2}\right)$, and the coefficients $\gamma_{j,s}$ are given (for $j = 0, 1$) by

$$\gamma_{j,s} = \frac{s!}{(2\pi i)^2} \oint_{\{0, \tau_c\}} \oint_{\{u(\tau)\}} \frac{(u - \alpha)^{a-1} u^{1-j} \left(\frac{1}{2} - \tau\right)^{b-1} \left(\frac{1}{2} + \tau\right)^{a-c}}{\left(\frac{1}{2}u^2 + \ln(1 - 4\tau^2)\right)^{s+1} (\tau - \tau_c)^a} du d\tau,$$

where $\tau_c = \frac{z-1}{2(z+1)}$. The τ -contour is a simple loop encircling the points 0 and τ_c , and, for each τ on this contour, the u -contour is a small loop encircling the point $u(\tau)$, where $\frac{1}{2}u^2 = -\ln(1 - 4\tau^2)$.

- **Expansion for ${}_2F_1(a + \lambda, b + 2\lambda; c; -z)$ as $\lambda \rightarrow \infty$ [70]:** For fixed $a, b, c \in \mathbb{C}$ and $|\arg z| < \pi$,

$${}_2F_1(a + \lambda, b + 2\lambda; c; -z) = (1+z)^{-\frac{3}{2}\lambda} \frac{\Gamma(c)\Gamma(1-c+b+2\lambda)}{\Gamma(b+2\lambda)} \times \left(\left[e^{(a-c+\lambda+\frac{1}{3})\pi i} \text{Ai}\left((e^{-\pi i}\lambda)^{2/3}x\right) + e^{-(a-c+\lambda+\frac{1}{3})\pi i} \text{Ai}\left((e^{\pi i}\lambda)^{2/3}x\right) \right] \chi_1 - \left[e^{(a-c+\lambda+\frac{2}{3})\pi i} \text{Ai}'\left((e^{-\pi i}\lambda)^{2/3}x\right) + e^{-(a-c+\lambda+\frac{2}{3})\pi i} \text{Ai}'\left((e^{\pi i}\lambda)^{2/3}x\right) \right] \chi_0 \right),$$

where

$$\chi_1 \sim \sum_{s=0}^\infty (-1)^s \gamma_{1,s} \lambda^{-s-\frac{1}{3}}, \quad \chi_0 \sim \sum_{s=0}^\infty (-1)^s \gamma_{0,s} \lambda^{-s-\frac{2}{3}},$$

as $\lambda \rightarrow \infty$ in $|\arg \lambda| \leq \frac{\pi}{2} - \delta < \frac{\pi}{2}$. Recall that $\text{Ai}(z)$ is the Airy function (see Appendix C). In the above equations, x is defined such that $\frac{4}{3}x^{3/2} = -2\zeta +$

$3 \log \left(\frac{2+e^\zeta}{2+e^{-\zeta}} \right)$, where $\zeta = \operatorname{arccosh} \left(\frac{1}{4}z - 1 \right)$; this implies that $z > 8 \Leftrightarrow \zeta > 0 \Leftrightarrow x > 0$. Additionally, the coefficients $\gamma_{j,s}$ are given (for $j = 0, 1$) by

$$\gamma_{j,s} = \frac{(-1)^s s!}{(2\pi i)^2} \oint_{\{\operatorname{sp}_\pm\}} \oint_{\{u(t)\}} \frac{t^{c-b-1} (t-1)^{a-c} (z+1-t)^{-a} u^j}{\left(\frac{1}{3}u^3 - xu + \gamma - \ln \left(\frac{t-1}{t^2(z+1-t)} \right) \right)^{s+1}} du dt,$$

where $\gamma = -\frac{3}{2} \ln(z+1)$. The t -contour is a simple loop encircling the saddle points $\operatorname{sp}_\pm := 2 + e^{\pm\zeta}$, and, for each t on this contour, the u -contour is a small loop encircling the point $u(t)$, where $\frac{1}{3}u^3 = \ln \left(\frac{t-1}{t^2(z+1-t)} \right) + xu - \gamma$ [70].

Using uniform asymptotic expansions to compute \mathbf{F} is more helpful than doing so for \mathbf{M} because the parameters are allowed to take complex values in the present expansions. The expansions for \mathbf{F} can be used if one chooses a, b, c , and λ so that the coefficients in the series expansions (which each entail either evaluating a contour integral or carrying out numerical differentiation) and the other special functions involved (which are detailed in Appendix C) can be evaluated accurately. However, computing these functions is itself an expensive process, even if accurate results can be obtained, so we believe uniform asymptotic expansions are likely to yield a potent numerical method only if convergence occurs after computation of very few terms of the series.

Additional research has been carried out on uniform asymptotic expansions for Gauss hypergeometric functions (for example, in [46, 71]), and [92] has a very useful summary of asymptotic results for these functions. Moreover, the Taylor series expansion (4.1) can be viewed as an asymptotic expansion for large values of $|c|$ and bounded a, b, z , and the expansion is particularly useful in this parameter regime.

4.7 Other methods for computing \mathbf{F}

Several other methods have been documented for the computation of $\mathbf{F}(a, b; c; z)$ [80]. For example, alternative methods can be used to compute the integral representation (4.4); these include splitting the integral, Romberg integration, and adaptive quadrature (though note that the latter two require that the integrand does not blow up at on either end point of the region of integration). Other possible methods include Padé approximants [83], evaluating a continued-fraction representation [115] using the technique described in Ref. [3], rational approximation [55], Chebyshev expansion [56], an ϵ -expansion method [42], exploiting alternative series expansions [52], and developing relationships between different types of hypergeometric functions by evaluating Feynman path integrals [47].

4.8 Summary and discussion

To compute $\mathbf{F}(a, b; c; z)$, we have considered several types of techniques—including Taylor series methods in Section 4.2, the single-fraction method in Section 4.2.1, and quadrature methods in Sections 4.3 and 4.7. In addition, we applied transformations

and analytic-continuation formulas from Sections 4.4 and 4.5 to find ways to compute F accurately and efficiently for all $z \in \mathbb{C}$.

We find that the series methods compute $F(a, b; c; z)$ accurately for values of $|a|$ and $|b|$ less than about 50. The single-fraction method is particularly useful when $|c| < 1$ and $|a|, |b| < 30$. When $\text{Re}(c) > \text{Re}(b) > 0$ or $\text{Re}(c) > \text{Re}(a) > 0$, the method based on Gauss-Jacobi quadrature is often effective. A variety of the above methods work well if $|z| \lesssim 0.9$.

A difficulty arises when one needs to compute values of $F(a, b; c; z)$ outside the unit disk $\{|z| = 1\}$. In such situations, one can apply the transformation formulas of Section 4.4 or the methods detailed therein for the special cases satisfying $b - a \in \mathbb{Z}$ or $c - a - b \in \mathbb{Z}$. A further issue arises when $|\text{Re}(a)|, |\text{Re}(b)|, \text{ or } |\text{Re}(c)|$ is too large for a method to work effectively on its own. (As a rough guide, this can occur when any of these values exceeds 50.) In such cases, one can exploit the recurrence-relation techniques of Section 4.6.1. Alternatively, one can employ the uniform asymptotic expansions of Section 4.6.2 if $|a|, |b|, \text{ or } |c|$ is large.

Table 6 Recommendations for which methods to use for computation of the Gauss hypergeometric function for real parameters and a real variable z satisfying $|z| < 1$. For $|z| \geq 1$, appropriate transformations are also necessary (see Section 4.4)

Case	Regions for a, b, c, z	Recommended method(s)	Relevant sections and references
I(A)	$a, b, c \geq 0, z \geq 0$	Taylor series methods; Single-fraction method; Gauss–Jacobi quadrature, if $c > b > 0$; Uniform asymptotic expansions for large parameter values	4.2 [3, 63] 4.2.1 [64, 65] 4.3 [26] 4.6.2 [69, 70, 99]
I(B)	$a, b, c \geq 0, z < 0$	Recurrences to combat cancellation, then Taylor series or single-fraction method	4.6.1 [14, 22, 24, 26, 28, 93] 4.2 [3, 63] 4.2.1 [64, 65]
II	$a, b < 0, c \geq 0$	Transformation (4.12), then same as for case I	4.8 [110, Eq. (15.8.1)]
III	$a, b \geq 0, c < 0$	Recurrence relations, then Taylor series or single-fraction method	4.6.1 [14, 22, 24, 26, 28, 93] 4.2 [3, 63] 4.2.1 [64, 65]
IV	$a, b, c < 0$	Transformation (4.12), then same as for case III	4.8 [110, Eq. (15.8.1)]
V	Either a or $b < 0$, $c \geq 0$	Recurrence relations, then Taylor series or single-fraction method	4.6.1 [14, 22, 24, 26, 28, 93] 4.2 [3, 63] 4.2.1 [64, 65]
VI	Either a or $b < 0$, $c < 0$	Recurrence relations, then same as for case V	4.6.1 [14, 22, 24, 26, 28, 93]

To devise an algorithm for cases in which all of the parameters and the variable are real, we follow the same type of procedure as for M . Namely, we apply forward

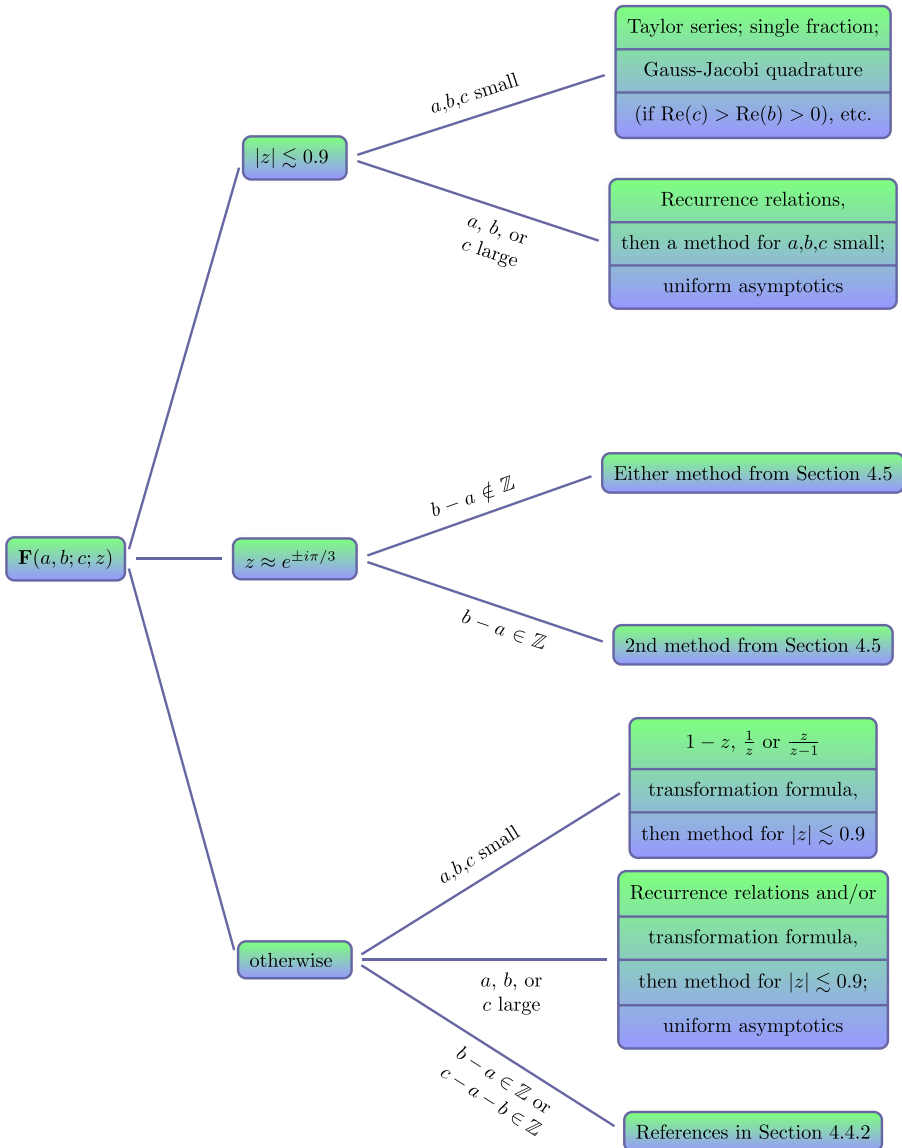


Fig. 8 Summary of recommended methods for computing F for different values of the parameters a, b , and c and the variable z . (The “etc.” in the upper right signifies that one can also use other methods from Section 4.7; a “large” parameter can refer either to its real part being large or to its absolute value being large, and an analogous comment holds for the adjective “small”. See the text for details)

recurrences to c so that all computations involve large values of $|c|$ and then use an additional transformation, such as [110, Eq. (15.8.1)]

$$\begin{aligned}
 {}_2F_1(a, b; c; z) &= (1 - z)^{c-a-b} {}_2F_1(c - a, c - b; c; z) & (4.12) \\
 \Leftrightarrow \mathbf{F}(a, b; c; z) &= (1 - z)^{c-a-b} \mathbf{F}(c - a, c - b; c; z)
 \end{aligned}$$

or the relation (4.6). We detail our strategy for the real case in Table 6.

When one extends the parameters and the variable into the complex plane, the problem of computing the Gauss hypergeometric function becomes more complicated. One can achieve good results when computing \mathbf{F} by following the procedure detailed in Fig. 8, which takes account of different values of $|a|$, $|b|$, $|c|$, and $|z|$.

Details of other software written to compute the Gauss hypergeometric function can be found in Refs. [23, 41, 53, 61, 62].

5 Concluding remarks

The confluent and Gauss hypergeometric functions arise in a large and diverse set of applications, and many other functions are special cases of them. However, both of these hypergeometric functions are notoriously difficult to compute effectively.

In this review paper, we have briefly outlined the theory of these hypergeometric functions, and we detailed a large number of good methods for computing them for different parameter and variable regimes. We have aimed to provide a roadmap for computing these functions for anyone who wishes to use them in a specific application and requires an effective implementation strategy for their evaluation.

There is no one method that provides a panacea for computing either \mathbf{M} or \mathbf{F} , as there are numerous difficult computational issues (such as cancellation and overflow). Accordingly, we have detailed numerous good methods that should be chosen carefully depending on the values of the parameters a and b (and also c for \mathbf{F}), and the variable z . We have included roadmaps for the computation of both \mathbf{M} and \mathbf{F} that should be used with appropriate transformations and recurrence relations (which we have also detailed). It is important to note that error bounds for the majority of these methods have not been widely researched (as most of the methods involve known series representations and hence can be calculated to arbitrary precision in infinite-precision arithmetic), but we believe the methods that we recommend have good error properties in the specified parameter and variable regions.

We have written and posted software for computing $\mathbf{M}(a; b; z)$ and $\mathbf{F}(a, b; c; z)$ [116]. We find the methods that we include in the software for computing \mathbf{M} to be effective for $|a|, |b|, |z| \lesssim 100$ for real parameters and variables, and for $|a|, |b|, |z| \lesssim 70$ for complex variables and parameters; the methods for computing \mathbf{F} are effective for $|a|, |b|, |c| \lesssim 100$ and for any z if the parameters and variables are real, and for $|a|, |b|, |c| \lesssim 70$ and for any z if they are complex. The methods are potent despite the fact that the code is implemented in double-precision arithmetic, in contrast to the majority of widely used software for hypergeometric functions. There are also other parameter and variable regimes for which our software can be applied

effectively—for instance, for large $|z|$ when computing \mathbf{M} —and we are currently developing the software to expand the parameter and variable regimes for which it is effective.

Acknowledgments This research was conducted over a number of years, beginning as a project in the University of Oxford’s MSc program in Mathematical Modelling and Scientific Computing so that the Numerical Algorithms Group (NAG) would be able to acquire enough information on the subject of computation of hypergeometric functions to achieve their goal of writing packages on the topic for the NAG Library [113]. The routines `s22ba` and `s22bb` (for computing confluent hypergeometric functions) and `s22be` and `s22bf` (for the Gauss hypergeometric functions) in the NAG library are based substantially on the work in this paper and the associated MSc project. We thank the staff at NAG—especially Mick Pont, David Sayers, and Lawrence Mulholland—for productive discussions. We also thank Andy Wathen and Nick Trefethen for useful advice. We also thank Frank Olver for providing us with an advanced copy of drafts of the chapters on hypergeometric functions in Ref. [110]. We are grateful to the many scientists who have contacted us about this work and have brought new applications of hypergeometric functions to our attention. JWP thanks the Engineering and Physical Sciences Research Council (EPSRC) and NAG for funding. We express our gratitude to the anonymous referees for their valuable comments.

Appendix A Test cases for \mathbf{M} and \mathbf{F}

This appendix details the test cases for \mathbf{M} and \mathbf{F} that we use in our numerical experiments in Appendix B. We show the test cases for \mathbf{M} in Table 7 and the test cases for \mathbf{F} in Table 8.

In addition to using test cases such as these, other methods can also be used to test the accuracy of our computations. For instance, one can use tabulated values from sources such as Refs. [90, 91, 108], test against known relations to elementary or special functions [3, 7, 57, 110], or test against known recurrence relations [3, 15, 34, 110] or Wronskians [56, 96, 110].

Appendix B Table of results for \mathbf{M} and \mathbf{F}

In this appendix, we present numerical results that indicate the number of digits of accuracy that we obtained when using a variety of methods for computing \mathbf{M} and \mathbf{F} .

In Table 9, we show results that we obtained when computing \mathbf{M} (or ${}_1F_1$ for values of b such that $\Gamma(b)$ is infinite in finite precision) for the two Taylor series methods of Section 3.2, the single-fraction method of Section 3.2.1, the Buchholz polynomial method of Section 3.3, the two methods for computing the asymptotic series of Section 3.4, and the Gauss–Jacobi quadrature method of Section 3.5.

In Table 10, we present results that we obtained for computing \mathbf{F} (or ${}_2F_1$ when c is such that $\Gamma(c)$ is infinite in finite precision) using the two Taylor series methods of Section 4.2, the single-fraction method of Section 4.2.1, the Gauss–Jacobi quadrature method of Section 4.3, and (in the column labeled “Bühning”) the analytic-continuation formula (4.10) of Section 4.5.

The label “A” in Tables 9 and 10 indicates that the series method in consideration did not converge after computing 500 terms. The label “B” indicates that the method was not effective because of overflow. The label “C,” which we use

Table 7 List of 40 test cases that we use to generate the results for **M** in Appendix B. The justification for the selection of these cases is given in Ref. [80]

Case	(a, b, z)	Case	(a, b, z)
1	$(0.1, 0.2, 0.5)$	21	$(20, -10 + 10^{-9}, -2.5)$
2	$(-0.1, 0.2, 0.5)$	22	$(20, 10 - 10^{-9}, 2.5)$
3	$(0.1, 0.2, -0.5 + i)$	23	$(-20, -10 + 10^{-12}, 2.5)$
4	$(1 + i, 1 + i, 1 - i)$	24	$(50, 10, 200i)$
5	$(10^{-8}, 10^{-8}, -10^{-10})$	25	$(-5, (-5 + 10^{-9})(1 + i), -1)$
6	$(10^{-8}, 10^{-12}, -10^{-10} + 10^{-12}i)$	26	$(4, 80, 200)$
7	$(1, 1, 10 + 10^{-9}i)$	27	$(-4, 500, 300)$
8	$(1, 3, 10)$	28	$(5, 0.1, -2 + 300i)$
9	$(500, 511, 10)$	29	$(-5, 0.1, 2 + 300i)$
10	$(8.1, 10.1, 100)$	30	$(2 + 8i, -150 + i, 150)$
11	$(1, 2, 600)$	31	$(5, 2, 100 - 1000i)$
12	$(100, 1.5, 2.5)$	32	$(-5, 2, -100 + 1000i)$
13	$(-60, 1, 10)$	33	$(-5, -2 - i, 1 + (2 - 10^{-10})i)$
14	$(60, 1, 10)$	34	$(1, 10^{-12}, 1)$
15	$(60, 1, -10)$	35	$(10, 10^{-12}, 10)$
16	$(-60, 1, -10)$	36	$(1, -1 + 10^{-12}i, 1)$
17	$(1000, 1, 10^{-3})$	37	$(1000, 1, -1000)$
18	$(10^{-3}, 1, 700)$	38	$(-1000, 1, 1000)$
19	$(500, 1, -5)$	39	$(-10 + 500i, 5i, 10)$
20	$(-500, 1, 5)$	40	$(20, 10 + 1000i, -5)$

sometimes when we present a result from Gauss–Jacobi quadrature, indicates that the test case in question is not in a valid parameter regime for the method to be applicable.

Appendix C Other special functions involved

To provide a comprehensive survey of the available methods for computing **M** and **F**, we also need to consider the computation of other special functions that arise along the way. The most common such function is the Gamma function, which is required for several of the methods to compute **M** (see Sections 3.3, 3.4, 3.5, 3.6, and 3.7) and **F** (see Sections 4.3, 4.4, 4.5, 4.6.1, 4.6.2, and 4.7). Two other germane special functions are the incomplete gamma function, whose computation is necessary for the hyperasymptotic series in Section 3.4, and the Bessel function, whose computation is necessary for the Buchholz polynomial method of Section 3.3 and for the theory of uniform asymptotics. The psigamma, Airy, and parabolic cylinder functions arise in the uniform asymptotic theory of Section 4.6.2. These special functions are discussed in more detail in Refs. [34, 73], and we note that the incomplete gamma and parabolic cylinder functions are themselves special cases of **M**, the Airy function is a special

Table 8 List of 30 test cases that we use to generate the results for **F** in Appendix B. The justification for the selection of these cases is given in Ref. [80]

Case	(a, b, c, z)	Case	(a, b, c, z)
1	(0.1, 0.2, 0.3, 0.5)	16	(−100, −200, −300 + 10 ^{−9} , 0.5√2)
2	(−0.1, 0.2, 0.3, 0.5)	17	(300, 10, 5, 0.5)
3	(0.1, 0.2, −0.3, −0.5 + 0.5i)	18	(5, −300, 10, 0.5)
4	(10 ^{−8} , 10 ^{−8} , 10 ^{−8} , 10 ^{−6})	19	(10, 5, −300.5, 0.5)
5	(10 ^{−8} , −10 ^{−6} , 10 ^{−12} , −10 ^{−10} + 10 ^{−12} i)	20	(2 + 200i, 5, 10, 0.6)
6	(1, 10, 1, 0.5 + 10 ^{−9} i)	21	(2 + 200i, 5 − 100i, 10 + 500i, 0.8)
7	(1, −1 + 10 ^{−12} i, 1, −0.8)	22	(2, 5, 10 − 500i, −0.8)
8	(2 + 8i, 3 − 5i, √2 − πi, 0.75)	23	(2.25, 3.75, −0.5, −1)
9	(100, 200, 350, i)	24	(1, 2, 4 + 3i, 0.6 − 0.8i)
10	(2 + 10 ^{−9} , 3, 5, −0.75)	25	(1, 0.9, 2, e ^{iπ/3})
11	(−2, −3, −5 + 10 ^{−9} , 0.5)	26	(1, 1, 4, e ^{iπ/3})
12	(−1, −1.5, −2 − 10 ^{−15} , 0.5)	27	(−1, 0.9, 2, e ^{−iπ/3})
13	(500, −500, 500, 0.75)	28	(4, 1.1, 2, 0.5 + (0.5√3 − 0.01)i)
14	(500, 500, 500, 0.75)	29	(5, 2.2, −2.5, 0.49 + 0.5√3i)
15	(−1000, −2000, −4000.1, −0.5)	30	(² / ₃ , 1, ⁴ / ₃ , e ^{iπ/3})

case of **M**, and the Bessel function is closely related to the *confluent hypergeometric limit function* ${}_0F_1$ [110].⁶

The inbuilt MATLAB routines for computing special functions (as of Version R2015a) are far from exhaustive; there only exist routines for the Gamma, Bessel, incomplete gamma, and Airy functions; and (apart from the Airy functions) these routines are usable only for a rather limited set of parameter and variable values. We therefore needed to use other routines to compute these functions accurately and efficiently for various parameter regions.

There is an inbuilt routine (`gamma`) for computing the Gamma function $\Gamma(z)$ in MATLAB, but it requires the argument z to be real. The NAG Library [113], however, contains a routine (`s14ag`) to evaluate $\log[\Gamma(z)]$ for any complex z , and we used this for some of our work. If one wishes to write his/her own routine for evaluating $\Gamma(z)$ for $z \in \mathbb{C}$, then for various values of z , one can use the Lanczos expansion [49] (possibly using an expansion given by Godfrey at [37]), Stirling expansions [3], Spouge’s method [89], or a Talbot contour method [86, 101, 105, 106]. When $\text{Re}(z) < \frac{1}{2}$ and $z \notin \mathbb{Z}$, the transformation [110, Eq. (5.5.3)]

$$\Gamma(z)\Gamma(1 - z) = \frac{\pi}{\sin(\pi z)}$$

may be helpful when using the Talbot contour method.

⁶We define the confluent hypergeometric limit function ${}_0F_1$ as follows:

$${}_0F_1(-; a; z) = \sum_{j=0}^{\infty} \frac{1}{(a)_j} \frac{z^j}{j!}.$$

Table 9 Table of results for various methods described in Section 3 for computing **M**. We state the number of digits of accuracy obtained by applying each method to each test case from Table 7 in Appendix A

Case	Taylor (a)	Taylor (b)	Single fraction	Buchholz	Asymptotic (a)	Asymptotic (b)	Gauss–Jacobi
1	16	16	16	A	A	A	16
2	16	16	16	16	A	A	C
3	16	16	16	A	A	A	15
4	16	16	15	15	A	A	C
5	16	16	15	9	A	A	C
6	8	15	15	0	A	A	C
7	15	16	15	5	A	A	C
8	15	15	15	15	16	16	14
9	16	16	15	A	A	A	B
10	15	16	0	13	15	15	13
11	A	A	0	A	16	16	12
12	16	15	15	15	A	A	C
13	0	0	0	14	A	A	C
14	15	15	15	15	A	A	C
15	0	0	0	15	A	A	C
16	16	16	16	15	A	A	C
17	16	16	16	16	A	A	C
18	A	A	0	A	16	16	13
19	0	0	0	16	A	A	C
20	0	0	0	15	A	A	C
21	6	6	6	8	A	A	C
22	16	16	15	8	A	A	C
23	5	5	5	8	A	A	C
24	0	0	B	A	A	A	C
25	14	14	14	15	A	A	C
26	15	16	0	A	15	15	0
27	14	14	14	A	A	A	C
28	0	0	B	A	14	14	C
29	14	15	15	A	14	14	C
30	A	0	A	A	B	B	C
31	A	A	B	A	15	15	C
32	15	15	15	A	15	15	C
33	0	15	15	A	A	A	C
34	4	15	16	12	A	A	C
35	4	15	15	11	A	A	C
36	15	15	15	0	A	A	C
37	A	A	0	A	A	A	C
38	A	A	0	A	A	A	C
39	A	1	A	0	A	A	C
40	16	16	15	A	A	A	C

We obtained these results using MATLAB R2015a. We note again that the label “A” indicates non-convergence of a series method, the label “B” indicates that the method was not effective because of overflow, and the label “C” indicates that the test case in question is not in the valid parameter regime for the Gauss–Jacobi quadrature method

MATLAB also has an inbuilt routine to compute the Bessel function $J_\nu(z)$, but it is only applicable for real ν , so it would be useful to design a routine that can also be used for complex ν . Such a routine could then be used for the methods in Sections

Table 10 Table of results for various methods described in Section 4 for computing **F**. We state the number of digits of accuracy obtained by applying each method to each test case from Table 8 in Appendix A

Case	Taylor (a)	Taylor (b)	Single fraction	Gauss–Jacobi	Bühning
1	16	16	16	16	A
2	16	16	16	15	A
3	16	16	16	C	16
4	15	15	15	C	A
5	16	16	16	C	12
6	15	15	15	C	A
7	16	16	15	C	A
8	14	15	A	C	A
9	A	A	A	B	A
10	16	16	15	16	0
11	8	8	8	C	A
12	16	16	16	C	A
13	0	0	0	C	A
14	A	A	B	C	A
15	14	14	0	C	A
16	0	0	0	C	A
17	A	A	0	C	A
18	0	0	0	13	A
19	0	0	0	C	A
20	0	0	B	6	A
21	3	3	A	B	A
22	16	16	16	B	A
23	A	A	0	C	16
24	A	A	A	C	A
25	A	A	3	14	11
26	A	A	5	14	11
27	16	16	16	15	16
28	A	A	A	14	16
29	A	A	A	C	14
30	A	A	A	15	16

We obtained these results using MATLAB R2015a. We note again that the label “A” indicates non-convergence of a series method, the label “B” indicates that the method was not effective because of overflow, and the label “C” indicates that the test case in question is not in the valid parameter regime for the Gauss–Jacobi quadrature method

3.3 and 4.6.2. In constructing such a code, one may wish to take advantage of its Taylor series, Hankel asymptotic representation, and integral relations [3], as well as work on practical computation of this function in [30]; and we exploit these tools in our code.

The “upper” and “lower” incomplete gamma functions $\Gamma(a, z)$ and $\gamma(a, z)$ can be computed for any complex z using the inbuilt MATLAB function `gammainc`, but this routine can only be applied for real $a \geq 0$. One hence needs to generalize this routine to implement the hyperasymptotic expansions detailed in Section 3.4. To do this, one can exploit Taylor series methods [83], asymptotic expansions [3], continued-fraction representations [83], recurrence relations [3], and the relation [110, Eq. (8.2.3)]

$$\gamma(a, z) + \Gamma(a, z) = \Gamma(a)$$

for $a \notin \mathbb{Z}^- \cup \{0\}$. A computational procedure for the evaluation of $\Gamma(a, z)$ and $\gamma^*(a, z) := \frac{\gamma(a, z)}{\Gamma(a)}$ is discussed in Ref. [25], and details of algorithms for $\gamma^*(a, z)$ and $\Gamma^*(a, z) := \frac{\Gamma(a, z)}{\Gamma(a)}$ are in Ref. [31].

The parabolic cylinder function $U(a, x)$ has yet to be implemented either in MATLAB or in the NAG Library. A routine for computing this function could exploit Maclaurin series, asymptotic series, and recurrence relations [34]; solving the underlying differential equation numerically [3]; and other strategies [94]. We also highlight articles that consider the practical computation of parabolic cylinder functions in [32, 35]. For the Airy function $\text{Ai}(z)$ and its derivative $\text{Ai}'(z)$ (which are closely related to the Bessel function [3]) and the psigamma function $\psi(z) = \frac{\Gamma'(z)}{\Gamma(z)}$, we use the NAG Library routines `s17dg` and `s14af`, respectively [113]; and we also highlight work carried out in [29].

Appendix D Recurrence relations used in Section 4.6.1

In this appendix, we state the recurrence relations for ${}_2F_1$ that we denoted in Section 4.6.1 as $(++0)$, $(00+)$, $(++-)$, and $(+0-)$. In addition to the relations themselves, we also indicate their minimal solutions (see Table 5) that inspire these notations. We discussed their regions of validity in Section 4.6.1. The recurrence relations and their solutions are as follows:

$(++0)$: **Recurrence:** $(c - a - n)(c - b - n)(c - a - b - 2n - 1)y_{n-1} + (c - a - b - 2n)[c(a + b - c + 2n) + c - 2(a + n)(b + n) + z\{(a + b + 2n)(c - a - b - 2n) + 2(a + n)(b + n) - c + 1\}]y_n + (a + n)(b + n)(c - a - b - 2n + 1)(1 - z)^2y_{n+1} = 0,$

Solution: $y_n = {}_2F_1(a + n, b + n; c; z),$

$(00+)$: **Recurrence:** $(c + n)(c + n - 1)(z - 1)y_{n-1} + (c + n)[c + n - 1 - \{2(c + n) - a - b - 1\}z]y_n + (c - a + n)(c - b + n)zy_{n+1} = 0,$

Solution: $y_n = {}_2F_1(a, b; c + n; z),$

$$\begin{aligned} \underline{(+ + -)} : \text{Recurrence: } & -(a - c + 2n)(a - c + 2n - 1)(b - c + 2n - 1)(b - c + 2n)zUy_{n-1} \\ & + (c - n)(c_1U + c_2V + c_3UV)y_n \\ & + (a + n)(b + n)(c - n)(c - n - 1)(1 - z)^3Vy_{n+1} = 0, \end{aligned}$$

$$\begin{aligned} \text{where } c_1 &= (1 - z)(b - c)(b - 1)[a - 1 + z(b - c - 1)], \\ c_2 &= b(b - c + 1)(1 - z)[a + z(b - c + 2)], \\ c_3 &= c - 2b - (a - b)z, \\ U &= z(a + b - c + 1)(a + b - c + 2) + ab(1 - z), \\ V &= (1 - z)(1 - a - b + ab) + z(a + b - c - 1)(a + b - c - 2), \end{aligned}$$

$$\text{Solution: } y_n = {}_2F_1(a + n, b + n; c - n; z),$$

$$\begin{aligned} \underline{(+ 0 -)} : \text{Recurrence: } & z(a - c + 2n)(a - c + 2n - 1)(b - c + n)[a + n + z(b - c + n + 1)]y_{n-1} \\ & + (c - n)[(a + n)(a + n - 1)(c - n - 1) \\ & + (a + n)(a + n - 1)(a + 3b - 4c + 5n + 2)z \\ & + (b - c + n)(b - c + n + 1)(4a - c + 5n - 1)z^2 \\ & - (a - b + n)(b - c + n)(b - c + n + 1)z^3]y_n \\ & - (a + n)(c - n)[a + n - 1 + z(b - c + n)](1 - z)^2y_{n+1} = 0, \end{aligned}$$

$$\text{Solution: } y_n = {}_2F_1(a + n, b; c - n; z).$$

References

1. Abad, J., Sesma, J.: Buchholz polynomials: A family of polynomials relating solutions of confluent hypergeometric and Bessel equations. *J. Comput. Appl. Math.* **101**, 237–241 (1999)
2. Abad, J., Sesma, J.: Computation of the regular confluent hypergeometric function. *The Mathematica Journal* **5**, 74–76 (1995)
3. Abramowitz, M., Stegun, I. (eds.): *Handbook of Mathematical Functions with Formulas, Graphs, and Mathematical Tables*. National Bureau of Standards (1970)
4. Allasia, G., Besenghi, R.: Numerical computation of Tricomi's psi function by the trapezoidal rule. *Computing* **39**, 271–279 (1987)
5. Ancarani, L.U., Gasaneo, G.: Derivatives of any order of the confluent hypergeometric function ${}_1F_1(a, b, z)$ with respect to the parameter a or b . *J. Math. Phys.* **49** (2008)
6. Andrews, G.E., Askey, R., Roy, R.: *Special Functions*, vol. 71 of *Mathematics and its Applications*. Cambridge University Press (1999)
7. Badrale, R., Marksteiner, P., Oh, Y., Freeman, A.J.: Computation of the Kummer functions and Whittaker functions by using Neumann type series expansions. *Comput. Phys. Commun.* **71**, 47–55 (1992)
8. Bell, K.L., Scott, N.S.: Coulomb functions (negative energies). *Comput. Phys. Commun.* **20**, 447–458 (1980)
9. Berry, M.V.: Asymptotics, superasymptotics, hyperasymptotics... In: *Asymptotics Beyond All Orders*, ed. H. Segur, S. Tanveer (Plenum, New York, 1991), pp. 1–14 (1992)
10. Boyle, P., Potapchik, A.: Application of high-precision computing for pricing arithmetic Asian options, pp. 39–46. *International Conference on Symbolic and Algebraic Computation* (2006)
11. Bühring, W.: An analytic continuation of the hypergeometric series. *SIAM J. Math. Anal.* **18**, 884–889 (1987)
12. Bühring, W.: An analytic continuation formula for the generalized hypergeometric function. *SIAM J. Math. Anal.* **19**, 1249–1251 (1988)
13. Chiochia, G., Gabutti, B.: A new transformation for computing hypergeometric series and the exact evaluation of the transonic adiabatic flow over a smooth bump. *Comput. Fluids* **17**, 13–23 (1989)

14. Deaño, A., Segura, J.: Transitory minimal solutions of hypergeometric recursions and pseudoconvergence of associated continued fractions. *Math. Comput.* **76**, 879–901 (2007)
15. Deaño, A., Temme, N.M.: On modified asymptotic series involving confluent hypergeometric functions. *Electron. Trans. Numer. Anal.* **35**, 88–103 (2009)
16. Dunster, T.M.: Asymptotic approximations for the Jacobi and ultraspherical polynomials, and related functions. *Methods Appl. Anal.* **6**, 21–56 (1999)
17. Dunster, T.M.: Uniform asymptotic expansions for Whittaker’s confluent hypergeometric function. *SIAM J. Math. Anal.* **20**, 744–760 (1989)
18. Eckart, C.: The penetration of a potential barrier by electrons. *Phys. Rev.* **35**, 1303–1309 (1930)
19. Efimov, A.: Intuitive model for the scintillations of a partially coherent beam. *Opt. Express* **22**, 32353–32360 (2014)
20. Erdélyi, A., Magnus, W., Oberhettinger, F., Tricomi, F.G.: *Higher Transcendental Functions*, vol. I. McGraw–Hill (1953)
21. Eremenko, V., Upadhyay, N.J., Thompson, I.J., Elster, C.h., Nunes, F.M., Arbanas, G., Escher, J.E., Hlophe, L.: Coulomb wave functions in momentum space. *Comput. Phys. Commun.* **187**, 195–203 (2015)
22. Ferreira, C., López, J.L., Sinusía, E.P.: The Gauss hypergeometric function $F(a, b; c; z)$ for large c . *J. Comput. Appl. Math.* **197**, 568–577 (2006)
23. Forrey, R.C.: Computing the hypergeometric function. *J. Comput. Phys.* **137**, 79–100 (1997)
24. Gautschi, W.: Computational aspects of three-term recurrence relations. *SIAM Rev.* **9**, 24–82 (1967)
25. Gautschi, W.: A computational procedure for incomplete gamma functions. *ACM Trans. Math. Softw.* **5**, 466–481 (1979)
26. Gautschi, W.: Gauss quadrature approximations to hypergeometric and confluent hypergeometric functions. *J. Comput. Appl. Math.* **139**, 173–187 (2002)
27. Gavrilá, M.: Elastic scattering of photons by a hydrogen atom. *Phys. Rev.* **163**, 147–155 (1967)
28. Gil, A., Segura, J., Temme, N.M.: The ABC of hyper recursions. *J. Comput. Appl. Math.* **190**, 270–286 (2006)
29. Gil, A., Segura, J.: Algorithm 819: AIZ, BIZ: Two Fortran 77 routines for the computation of complex Airy functions. *Trans. Math. Softw.* **28**, 325–336 (2002)
30. Gil, A., Segura, J.: Algorithm 831: Modified Bessel functions of imaginary order and positive argument. *Trans. Math. Softw.* **30**, 159–164 (2004)
31. Gil, A., Segura, J., Temme, N.M.: Efficient and accurate algorithms for the computation and inversion of the incomplete gamma function ratios. *SIAM J. Sci. Comput.* **34**, A2965–A2981 (2012)
32. Gil, A., Segura, J., Temme, N.M.: Fast and accurate computation of the Weber parabolic cylinder function $W(a, x)$. *IMA J. Numer. Anal.* **31**, 1194–1216 (2011)
33. Gil, A., Segura, J., Temme, N.M.: Numerically satisfactory solutions of hypergeometric recursions. *Math. Comput.* **76**, 1449–1468 (2007)
34. Gil, A., Segura, J., Temme, N.M.: *Numerical Methods for Special Functions*. Society for Industrial and Applied Mathematics (2007)
35. Gil, A., Segura, J., Temme, N.M.: Parabolic cylinder function $W(a, x)$ and its derivative. *ACM Trans. Math. Softw.* **38** (2011). Article 6
36. Glaser, A., Liu, X., Rokhlin, V.: A fast algorithm for the calculation of the roots of special functions. *SIAM J. Sci. Comput.* **29**, 1420–1438 (2007)
37. Godfrey, P.: A note on the computation of the convergent Lanczos complex gamma approximation (2001), available at <http://www.numericana.com/answer/info/godfrey.htm>
38. Golub, G.H., Welsch, J.W.: Calculation of Gauss quadrature rules. *Math. Comput.* **23**, 221–230 (1969)
39. Hale, N., Townsend, A.: Fast and accurate computation of Gauss–Legendre and Gauss–Jacobi quadrature nodes and weights. *SIAM J. Sci. Comput.* **35**, A652–A674 (2013)
40. Hochstadt, H.: *The Functions of Mathematical Physics*. Wiley (1971)
41. Hsu, Y.P.: Development of a Gaussian hypergeometric function code in complex domains. *Int. J. Modern Phys. C* **4**, 805–840 (1993)
42. Huang, H.-Z., Liu, J.: NumExp: Numerical epsilon expansion of hypergeometric functions. *Comput. Phys. Commun.* **184**, 1973–1980 (2013)
43. Ibrahim, A.K., Rakha, M.A.: Contiguous relations and their computations for ${}_2F_1$ hypergeometric series. *Comput. Math. Appl.* **56**, 1918–1926 (2008)

44. Jones, D.S.: Asymptotics of the hypergeometric function. *Math. Methods Appl. Sci.* **24**, 369–389 (2001)
45. Kalla, S.L.: On the evaluation of the Gauss hypergeometric function. *Compt. Rendus l'Acad. Bulgare Sci.* **45**, 35–36 (1992)
46. Khwaja, F., Olde Daalhuis, A.B.: Uniform asymptotic expansions for hypergeometric functions with large parameters IV. *Anal. Appl.* **12**, 667–710 (2014)
47. Kniehl, B.A., Tarasov, O.V.: Finding new relationships between hypergeometric functions by evaluating Feynman integrals. *Nuclear Phys. B* **854**, 841–852 (2012)
48. Korotkova, O.: Scintillation index of a stochastic electromagnetic beam propagating in random media. *Opt. Commun.* **281**, 2342–2348 (2008)
49. Lanczos, C.J.: A precision approximation of the gamma function. *SIAM J. Numer. Anal. Ser. B* **1**, 86–96 (1964)
50. López, J.L.: Asymptotic expansions of the Whittaker functions for large order parameter. *Methods Appl. Anal.* **6**, 249–256 (1999)
51. López, J.L., Pagola, P.J.: The confluent hypergeometric functions $M(a, b; z)$ and $U(a, b; z)$ for large b and z . *J. Comput. Appl. Math.* **233**, 1570–1576 (2010)
52. López, J.L., Temme, N.M.: New series expansions of the Gauss hypergeometric function. *Adv. Comput. Math.* **39**, 349–365 (2013)
53. Lozier, D.W., Olver, F.W.J.: Numerical evaluation of special functions. In: *Mathematics of Computation 1943–1993: A Half-Century of Computational Mathematics, Proceedings of Symposia in Applied Mathematics*, American Mathematical Society (1994)
54. Luke, Y.L.: Algorithms for rational approximations for a confluent hypergeometric function. *Utilitas Math.* **11**, 123–151 (1977)
55. Luke, Y.L.: *Algorithms for the Computation of Mathematical Functions*. Academic Press (1977)
56. Luke, Y.L.: *Mathematical Functions and their Approximations*. Academic Press (1975)
57. Luke, Y.L.: *The Special Functions and their Approximations, vol. I*. Academic Press (1969)
58. Luke, Y.L.: *The Special Functions and their Approximations, vol. II*. Academic Press (1969)
59. Mace, R.L., Hellberg, M.A.: A dispersion function for plasmas containing superthermal particles. *Phys. Plasmas* **2**, 2098–2109 (1995)
60. Mathar, R.J.: Numerical representations of the incomplete gamma function of complex-valued argument. *Numer. Algorithms* **36**, 247–264 (2004)
61. Michel, N., Stoitsov, M.V.: Fast computation of the Gauss hypergeometric function with all its parameters complex with application to the Pöschl–Teller–Ginocchio potential wave functions. *Comput. Phys. Commun.* **178**, 535–551 (2008)
62. Moshier, S.L.: *Methods and Programs for Mathematical Functions*. Ellis Horwood (1989)
63. Muller, K.E.: Computing the confluent hypergeometric function, $M(a, b, x)$. *Numer. Math.* **90**, 179–196 (2001)
64. Nardin, M., Perger, W.F., Bhalla, A.: Algorithm 707: CONHYP: A numerical evaluator of the confluent hypergeometric function for complex arguments of large magnitudes. *ACM Trans. Math. Softw.* **18**, 345–349 (1992)
65. Nardin, M., Perger, W.F., Bhalla, A.: Numerical evaluation of the confluent hypergeometric function for complex arguments of large magnitudes. *J. Comput. Appl. Math.* **39**, 193–200 (1992)
66. Nieuwveldt, F.D.: *A Survey of Computational Methods for Pricing Asian Options*. Masters' thesis, University of Stellenbosch (2009). available at <http://scholar.sun.ac.za/handle/10019.1/2118>
67. Noble, C.J., Thompson, I.J.: COULN, a program for evaluating negative energy coulomb functions. *Comput. Phys. Commun.* **33**, 413–419 (1984)
68. Olde Daalhuis, A.B.: Hyperasymptotic expansions of confluent hypergeometric functions. *IMA J. Appl. Math.* **49**, 203–216 (1992)
69. Olde Daalhuis, A.B.: Uniform asymptotic expansions for hypergeometric functions with large parameters I. *Anal. Appl.* **1**, 111–120 (2003)
70. Olde Daalhuis, A.B.: Uniform asymptotic expansions for hypergeometric functions with large parameters II. *Anal. Appl.* **1**, 121–128 (2003)
71. Olde Daalhuis, A.B.: Uniform asymptotic expansions for hypergeometric functions with large parameters III. *Anal. Appl.* **8**, 199–210 (2010)
72. Olde Daalhuis, A.B., Olver, F.W.J.: Hyperasymptotic solutions of second-order linear differential equations I. *Methods Appl. Anal.* **2**, 173–197 (1995)

73. Olver, F.W.J.: *Asymptotics and Special Functions*. Academic Press (1974)
74. Olver, F.W.J.: Exponentially-improved asymptotic solutions of ordinary differential equations I: the confluent hypergeometric function. *SIAM J. Math. Anal.* **24**, 756–767 (1993)
75. Olver, F.W.J.: Numerical solution of second order linear difference equations. *J. Res. Nat. Bur. Stand. Sect. B* **71**, 111–129 (1967)
76. Olver, F.W.J.: On the asymptotic solution of second-order differential equations having an irregular singularity of rank one, with an application to Whittaker functions. *J. Soc. Indust. Appl. Math. Ser. B (Numerical Analysis)* **2**, 225–243 (1965)
77. Olver, F.W.J.: Uniform, exponentially improved, asymptotic expansions for the confluent hypergeometric function and other integral transforms. *SIAM J. Math. Anal.* **22**, 1475–1489 (1991)
78. Olver, F.W.J.: Whittaker functions with both parameters large: uniform approximations in terms of parabolic cylinder functions. *Proc. Royal Soc. Edinb. Sect. A* **86**, 213–234 (1980)
79. Pastor-Satorras, R., Vespignani, A.: Epidemic dynamics and endemic states in complex networks. *Phys. Rev. E* **63**, 066117 (2001)
80. Pearson, J.: *Computation of Hypergeometric Functions*, Dissertation, MSc in Mathematical Modelling and Scientific Computing, University of Oxford (2009), available at <https://sites.google.com/site/johnpearsonmaths/research>
81. Pierro, V., Pinto, I.M., Spallicci di Filottrano, A.D.A.M.: Computation of hypergeometric functions for gravitationally radiating binary stars. *Mon. Not. Royal Astron. Soc.* **334**, 855–858 (2002)
82. Potts, P.J.: *Computable real arithmetic using linear fractional transformations*. Report, Department of Computing, Imperial College of Science, Technology and Medicine, London (1996), available at <http://citeseer.ist.psu.edu/potts96computable.html>
83. Press, W.A., Teukolsky, S.A., Vetterling, W.T., Flannery, B.P.: *Numerical Recipes: The Art of Scientific Computing*. 3rd edn. Cambridge University Press (2007)
84. Rakha, M.A., El-Sedy, E.S.: Application of basic hypergeometric series. *Appl. Math. Comput.* **148**, 717–723 (2004)
85. Roach, K.: Hypergeometric function representations, pp. 301–308. *Proceedings of the 1996 International Symposium on Symbolic and Algebraic Computation* (1996)
86. Schmelzer, T., Trefethen, L.N.: Computing the gamma function using contour integrals and rational approximations. *SIAM J. Numer. Anal.* **45**, 558–571 (2007)
87. Seaborn, J.B.: *Hypergeometric Functions and their Applications*. Springer-Verlag (1991)
88. Segura, J., Temme, N.M.: Numerically satisfactory solutions of Kummer recurrence relations. *Numer. Math.* **111**, 109–119 (2008)
89. Spouge, J.L.: Computation of the gamma, digamma, and trigamma functions. *SIAM J. Numer. Anal.* **31**, 931–944 (1994)
90. Slater, L.J.: *Confluent Hypergeometric Functions*. Cambridge University Press (1960)
91. Slater, L.J.: *Generalized Hypergeometric Functions*. Cambridge University Press (1966)
92. Temme, N.M.: *Asymptotic Methods for Integrals*. Series in Analysis 6, World Scientific, NJ (2015)
93. Temme, N.M.: Large parameter cases of the Gauss hypergeometric function. *J. Comput. Appl. Math.* **153**, 441–462 (2003)
94. Temme, N.M.: Numerical and asymptotic aspects of parabolic cylinder functions. *J. Comput. Appl. Math.* **121**, 221–246 (2000)
95. Temme, N.M.: Numerical aspects of special functions. *Acta Numer.* **16**, 379–478 (2007)
96. Temme, N.M.: The numerical computation of the confluent hypergeometric function $U(a, b, z)$. *Numer. Math.* **41**, 43–82 (1983)
97. Temme, N.M.: *Special Functions: An Introduction to the Classical Functions of Mathematical Physics*. Wiley (1996)
98. Temme, N.M.: Uniform asymptotic expansions of confluent hypergeometric functions. *J. Inst. Math. Appl.* **22**, 215–223 (1978)
99. Temme, N.M.: Uniform asymptotics for a class of integrals in terms of modified Bessel functions, with application to confluent hypergeometric functions. *SIAM J. Math. Anal.* **21**, 241–261 (1990)
100. Torrieri, D., Valenti, M.C.: The outage probability of a finite ad hoc network in Nakagami fading. *IEEE Trans. Commun.* **60**, 3509–3518 (2012)
101. Trefethen, L.N., Weideman, J.A.C., Schmelzer, T.: Talbot quadratures and rational approximations. *BIT. Numer. Anal.* **46**, 653–670 (2006)

102. Vitalis, R., Gautier, M., Dawson, K.J., Beaumont, M.A.: Detecting and measuring selection from gene frequency data. *Genetics* **196**, 799–814 (2014)
103. Wang, X., Duan, J., Li, X., Luan, Y.: Numerical methods for the mean exit time and escape probability of two-dimensional stochastic dynamical systems with non-Gaussian noises. *Appl. Math. Comput.* **258**, 282–295 (2015)
104. Watson, G.N.: The harmonic functions associated with the parabolic cylinder. *Proc. Lond. Math. Soc.* **2**, 116–148 (1918)
105. Weideman, J.A.C.: Optimizing Talbot’s contours for the inversion of the Laplace transform. *SIAM J. Numer. Anal.* **44**, 2342–2362 (2006)
106. Weideman, J.A.C., Trefethen, L.N.: Parabolic and hyperbolic contours for computing the Bromwich integral. *Math. Comput.* **76**, 1341–1356 (2007)
107. Wimp, J.: *Computation with Recurrence Relations*. Pitman (1984)
108. Zhang, S., Jin, J.: *Computation of Special Functions*. Wiley (1966)
109. Zhao, C., Yang, C.: An exact solution for electroosmosis of non-Newtonian fluids in microchannels. *J. Non-Newtonian Fluid Mech.* **166**, 1076–1079 (2011)
110. Digital Library of Mathematical Functions, National Institute of Standards and Technology, available at <http://dlmf.nist.gov/>
111. MATLAB, The Mathworks Inc., Version R2015a (2015)
112. Mathematica, Wolfram Research, Inc., Mathematica, Version 8.0 (2010)
113. The NAG Toolbox for MATLAB, The Numerical Algorithms Group (2013)
114. <http://functions.wolfram.com/HypergeometricFunctions/Hypergeometric1F1/10/>
115. <http://functions.wolfram.com/HypergeometricFunctions/Hypergeometric2F1/10/>
116. <http://datashare.is.ed.ac.uk/handle/10283/607>